Design and Development of a 100 W Proton Exchange Membrane Fuel Cell Uninterruptible Power Supply

Johannes Paulus du Toit

20416369

A dissertation submitted in fulfillment of the requirements for the Magister Technologiae: Engineering: Electrical

Department: Applied Electronics and Electronic Communication

Faculty of Engineering

Vaal University of Technology

Vanderbijlpark

Supervisor: Prof HCvZ Pienaar

Date: January 2006

Declaration

I, Johan du Toit, hereby declare that the following research information is solely my own work. This is submitted for the requirements of the Magister Technologiae: Engineering: Electrical to the Department of Applied Electronics and Electronic Communication at the Vaal University of Technology, Vanderbijlpark. This work has not previously been accepted in substance for any degree and is not being concurrently submitted in candidature for any degree.

Signed .....

Date 2006-04-24

Acknowledgements

- Prof HCvZ Pienaar for encouragement and guidance throughout this research.
- Mr JF Janse van Rensburg for his help in designing the PID controller algorithm.
- Personnel of the Department of Applied Electronics and Electronic Communication for support and encouragement.
- Telkom Center of Ecellence, TFMC, M-Tech and THRIP
- Prof P Mendonidis as language editor.

Abstract

This study presents the design of a proton exchange membrane fuel cell stack that can be used to replace conventional sources of electrical energy in an uninterruptible power supply system, specifically for use in the telecommunications industry. One of the major concerns regarding the widespread commercialization of fuel cells is the high cost associated with fuel cell components and their manufacturing. A fuel cell design is presented in which existing, low-cost, technologies are used in the manufacture of cell components. For example, printed circuit boards are used in the manufacturing of bipolar flow plates to significantly reduce the cost of fuel cells.

The first objective was to design, construct and test a single fuel cell and small fuel cell stack in order to evaluate the use of printed circuit boards in bipolar plate manufacturing. Since the use of copper in a fuel cell environment was found to reduce the lifetime of the cells, the bipolar plates were coated with a protective layer of nickel and chrome. These coatings proved to increase the lifetime of the cells significantly. Power outputs of more than 4 W per cell were achieved.

The second objective was to analyze a small fuel cell stack in order to obtain a model for predicting the performance of larger stacks. A mathematical model was developed which was then used to design an electronic circuit equivalent of a fuel cell stack. Both models were adapted to predict the performance of a fuel cell stack containing any number of cells. The models were proven to be able to accurately predict the performance of a fuel cell stack by comparing simulated results with practical performance data.

Finally, the circuit equivalent of a fuel cell stack was used to evaluate the capability of a switch mode boost converter to maintain a constant voltage when driven by a fuel cell stack, even under varying load conditions. Simulation results showed the ability of the boost converter to maintain a constant output voltage. The use of supercapacitors as a replacement for batteries as a secondary energy source was also evaluated.

TABLE OF CONTENTS

List of tables

Annexures

Glossary of abbreviations and symbols

A

A – Tafel constant

α - Charge transfer coefficient

AC – Alternating current

ADC – Analog to digital converter

B

β – Transistor current gain

BJT – Bipolar junction transistor

BP – Bipolar plate

C

C – Coulomb

C – Carbon

C – Celsius

Cu – Copper

cm – 10^{-2} meter

Cr – Chromium

CV – Control variable

D

ΔG_f – Change in gibbs free energy of formation

$\Delta \bar{g}_f$ - per mole change in gibbs free energy of formation

ΔV_{act} – Activation loss

ΔV_{ohm} – Ohmic loss

ΔV_{trans} – Mass transfer loss

DC – Direct current

D_k – Derivative term at time k

DMFC – Digital mass flow controller

DMFM – Digital mass flow meter

E

e_k – Error at time k

E – Theoretical fuel cell electromotive force

E_{OC} – Practical fuel cell open circuit voltage

EES – Electrical energy storage

EMF – Electromotive force

F

F – Farad

F – Faraday constant, 96 485 Coulomb

F – Fluorine

FA – Flashback arrestor

FC – Fuel cell

G

g – gram

G_f – Gibbs free energy of formation

GDL – Gas diffusion layer

H

H – Henry

H – Hydrogen atom

H^+ - Hydrogen proton or cation

H_2 – hydrogen molecule

H_2O – Water

I

i – Fuel cell stack output current density

i_0 – Exchange current density

i_n – Total internal current density

I_D – Current through a diode

I_O – Fuel cell stack output current

I_S – Saturation current of a transistor

I_{SD} – Saturation current of a diode

I_k – Integral term at time k

ICE – Internal combustion engine

J

J – Joule

K

k – Boltzmann's constant, 1.38 x 10^{-23} $J.K^{-1}$

K – Kelvin

K_D – Derivative gain constant

K_I – Integral gain constant

K_P – Proportional gain constant

L

λ – Stoichiometric flow rate

M

m – Mass-transfer overvoltage constant

m – Meter

m – Mili, 10^{-3}

mm – Milimeter

MEA – Membrane electrode assembly

MOSFET – Metal-oxide semiconductor field effect transistor

N

n – mass transfer overvoltage coefficient

n – Emission coefficient

N – Avogadro's number, 6.022 x 10^{23}

N – Newton

N_C – Number of cells in a fuel cell stack

NASA – National Aeronautical and Space Administration

Ni – Nickel

O

Ω - Ohm

O – Oxygen

P

P_1, P_2 – Pressure
P_{H2} – Hydrogen pressure
P_{H2O} – Water pressure
P_k – Proportional term at time k
P_{O2} – Oxygen pressure
Pa – Pascal
PCB – Printed circuit board
PEM – Proton exchange membrane
PEMFC – Proton exchange membrane fuel cell
PID – Proportional Integral Derivative
PTFE – Polytetrafluoroethelyne
PWM – Pulse-width modulation

Q

q – Charge of an electron, 1.602×10^{-19} C

R

R – Resistance
R – Universal gas constant, 8.314 $J.K^{-1}$ mol^{-1}
R_D – Ohmic resistance of a diode
r – Area specific resistance

S

S – Sulphur
SLPM – Standard liters per minute
SP – Set point

T

T – Absolute temperature
t_{OFF} – Off-time of a switch
t_{ON} – On-time of a switch

U

μ - micro, 10^{-6}
UPS – Uninterruptible power supply

V

V – Volt
V_D – Voltage across a diode
V_{DC} – Direct current voltage
V_{IN} – Input voltage
V_O – Output Voltage
V_{OUT} – Output voltage
V_S – Direct current cource voltage
V_{STACK} – Output voltage of a fuel cell stack
V_T – Thermal voltage

W

W – Watt

XYZ

Chapter 1 Introduction

1.1 Background

In recent years, there has been an increased demand in cheap, reliable and clean sources of energy. With the increasing amount of environmental pollution from internal combustion engines (ICEs) in cars, more manufacturers are now looking towards replacing these engines with an alternative, cleaner, source of energy. Governments of countries around the world have realized the severity of the problem and are now actively participating in replacing ICEs by funding research or with various forms of legislation.

Fossil fuels also play a big role in power generation for stationary applications and a number of alternative energy sources have been developed for this purpose. Solar panels and wind turbines can only generate energy under certain conditions and batteries are still needed to store the energy for times when there is no sunlight or wind. This leads to complex and expensive systems. Batteries require maintenance, have limited lifetimes, and contain toxic heavy metals that may cause serious environmental problems if discarded incorrectly. Portable electronic devices like cellphones and laptop computers also currently use batteries that have limited lifetimes and charge-discharge cycles.

Fuel cells (FCs) are a very attractive source of electrical energy for both stationary and mobile applications. In a fuel cell, a fuel and oxidant are converted into electricity via an electrochemical process. Since no combustion takes place, FCs are much more efficient and cleaner than ICEs. Since FCs contain no moving parts, they require less maintenance and have much longer lifetimes. Unlike batteries, FCs can supply energy for as long as it is being fed with fuel. Over recent years, a number of different FCs have been developed, each using different fuels and operating at various temperatures. One type of FC that has received much attention as a candidate for use in automobile, stationary and portable applications, is the proton exchange membrane fuel cell (PEMFC). PEMFCs are based on a solid proton conducting electrolyte and operates at temperatures less than 100 °C.

One of the major concerns regarding PEMFCs is the high manufacturing and materials costs. Over the past years, giant leaps have been made in reducing these costs, but some challenges still exist. In spite of these relatively high costs, FCs have already proven to be more cost efficient in the long run, compared to battery based systems.

1.2 Problem statement

One of the main stumbling blocks for FCs thus far has been the high material costs and manufacturing costs associated with FC components. Not only will low-cost components enable the widespread commercialization of FCs, but it will also have great benefits for future research. This means that a method must be found for producing low-cost FCs in a short time.

The current-voltage characteristics of a FC stack can also present a number of challenges when used in a UPS system. It is important that the output voltage of the UPS stays constant within a certain range, regardless of the current drawn. The system should also be able to handle rapid changes in load. Since the output voltage of a FC drops as more current is drawn from it, a DC voltage regulation circuit is crucial in maintaining a constant output voltage. It is also not possible for a FC stack to deliver maximum power instantaneously from an idle state. In order to enable the system to handle rapid changes in load, as well as compensating for the start-up time of a FC stack, some form of secondary energy storage must be included in the system. Since there are a number of disadvantages associated with the use of batteries as a secondary energy storage, the use of supercapacitors will be investigated as a replacement for batteries.

1.3 Methodology

The research commenced with a study of literature related to the design of PEMFC stacks, mathematical modeling of FCs, power converters and secondary energy storage devices. A small, two-cell, PEMFC stack was constructed and its voltage-current characteristics obtained. The resulting data was then used to construct and validate a mathematical model of the stack. The mathematical model was then used to design an electronic circuit equivalent of the FC stack. The mathematical model as well as the electronic circuit equivalent model were tested by comparing the calculated values of a four-cell stack with data obtained by testing an actual four-cell stack. Both models were then adapted to simulate the characteristics of a 100 W PEMFC stack.

In order to regulate the output voltage of the FC stack, a switch mode boost regulator was designed. A digital PID (Proportional Integral Derivative) controller was also designed in order to ensure a constant regulator output voltage at various load currents. A low-power, proof-of-concept, boost converter was then constructed and tested in order to evaluate the design. The

research concluded with the simulation of the 100 W FC stack using its electronic circuit equivalent together with the boost converter.

1.4 Delimitations

Both the mathematical model of the FC stack and its electronic circuit equivalent were based on the operation of the stack under constant conditions. The effects of variations in pressure, flow rate, temperature and humidity were not included in either of the two models. The final 100 W system was only evaluated using computer simulations. The models used in the simulations were extrapolated from, and validated with, small proof-of-concept prototypes. This research also did not consider the design of a bidirectional converter needed by the supercapacitors.

1.5 Importance of research

The result of this research is the design of a UPS system using FC technology that is able to deliver backup power in a much cheaper and more efficient way. The process by which energy is converted is entirely chemical in nature, and since the system will contain no moving parts, maintenance costs will decrease dramatically compared to that of a system based on a generator or even batteries. A low-maintenance system will be very beneficial to the telecommunications industry for use in remote sites. FCs are a very clean source of energy, making the system clean and environmentally friendly. The project will also result in a FC design that can be manufactured at a low cost and in little time. Short prototyping times of FCs can be very useful in research as well, since different cell designs and configuration can be manufactured and tested in a very short time.

1.6 Overview of the report

Chapter 2 starts with a discussion on the history of PEMFCs and their advantages. The characteristics of PEMFCs are also discussed together with the factors that contribute to these characteristics. A mathematical model based on the various sources of voltage losses in a FC is presented followed by a discussion on an electronic circuit equivalent of a FC stack. The latter can be used to simulate the FC together with peripheral electronic circuitry using an electronic simulation package. Chapter 2 concludes with a discussion on switch mode boost converters and secondary energy storage devices which are used to ensure a constant output voltage of a PEMFC UPS system.

In chapter 3, the actual design of a small PEMFC stack and switch mode boost converter are discussed in detail. The electronic circuit model and mathematical model of a PEMFC stack given in chapter 2 are further developed based on the operation of the PEMFC stack. Both of these models are compared to the actual performance data of a PEMFC stack in order to evaluate their accuracy. Chapter three concludes with an overview of the final PEMFC UPS system.

Chapter 4 describes the various measurements performed on the FC stack and boost converter. Performance data of a small PEMFC stack are presented and discussed. This chapter also discusses the computer simulations performed on the complete 100 W UPS system.

In chapter 5, conclusion are drawn from the study and recommendations are made regarding the design of a PEMFC UPS system.

1.7 Summary

This chapter presented the underlying reasons for the execution of the research as well as its importance and relevance, especially to the South African telecommunications industry. The methodology that was used in the research was described and an overview of the report was given. In chapter 2, the operation of a PEMFC stack together with various factors influencing its performance as well as the modeling of a PEMFC stack are discussed. Chapter 2 concludes with a discussion of the important principles regarding switch mode boost converters and secondary energy storage devices.

Chapter 2 Theoretical considerations of a PEMFC UPS system

2.1 Introduction

Since FCs found their first application in the 1960s in NASA's Gemini space flights, extensive research has been carried out by various organizations and institutions throughout the world in order to find a way to eliminate the use of fossil fuels as an energy source. Although the principle of a FC was discovered in as early as 1830 by Sir William Grove, it was only about 130 years later that FCs were first used to by NASA to supply electrical energy for their space craft and drinking water for the crew (Larmine & Dicks 2003:1-10).

A FC is an electrochemical device where the chemical energy contained in hydrogen (H_2) and oxygen (O_2) are converted directly into electrical energy, water and heat. Although the reactants for a FC are referred to as fuel, no combustion takes place and the process is entirely a chemical one. At the anode of a fuel cell, hydrogen gas is oxidized and is broken down into two protons (H^+) and two electrons (e^-). Only the protons can move through the electrolyte, leaving the external electric circuit connected to the fuel cell as the only path through which electrons can travel. At the cathode, oxygen reacts with electrons taken from the electrode, and H^+ ions from the electrolyte, to form water (Larmine & Dicks 2003:2). In a FC, the electrons flow from one electrode (anode) through an external electric circuit to the second electrode (cathode). The protons, one the other hand, move through the electrolyte.

Different types of fuel cells, characterized by the electrolyte that they use, are being developed and are all different in terms of the fuel that they use and operating temperature (Ledjeff-Hey *et al.* 1998:199). Because of its simplicity and low operating temperature, PEMFCs are ideal for implementation in mobile and lower power applications. According to Costamagna and Srinivasan (2001:242), PEMFCs are foremost among the different types of FCs, because of various environmental legislations in a number of countries. This stimulated a worldwide renaissance in the development of portable power and power generation applications. PEMFCs exhibit a high energy density at low operating temperatures (70 – 90 °C), quick start-up capability, zero emissions and minimal problems from component corrosion and electrolyte leakage compared to other types of fuel cells (Chu *et al.* 2003:1).

Earlier version of PEMFCs, as used by NASA in the 1960s, only had a lifetime of about 500 hours. In 1967, an American company called Dupont, started producing a material called Nafion,

which became a standard in PEMFCs and is still used today. The problem of water management in the electrolyte, together with the high costs associated with the manufacturing of PEMFCs hindered any further development during the 1970s and early 1980s. During that time, catalyst technology improved to such an extend that today, only about 0,2 mg of platinum per square centimeter is needed, compared to the 28 $mg.cm^{-2}$ needed in the late 1960s. Further developments in the materials used in PEMFCs have ensured its continued development as a power source for cars and portable applications (Larmine & Dicks 2003:67-68).

The main motivation for the development of FCs (in particular PEMFCs) with a power output of 1-200 kW for stationary and transportation applications is its environmental benefits. The motivation for developing small PEMFCs, up to hundreds of watts, resides in improved technical characteristics compared to established technologies which consist mainly of primary and secondary batteries. FCs have the advantage over batteries of higher energy densities and no recharging time. When designing small PEMFC systems, however, the issue of supplying electrical power to the system's ancillary components (for example, humidifiers, flow rate controllers and temperature controllers) becomes problematic since not enough power is available to drive these sub-systems, unlike the situation with larger FC systems. This requires a small PEMFC system to be operated with a minimized level of control (Jaouen *et al.* 2005:113-114).

FCs are not an energy source and must rather be seen as an energy conversion technology. Chemical energy contained in a fuel is converted into electricity with much higher efficiency than most of the existing chemical fuel-to-electricity technologies. Unlike internal combustion engines (ICEs), whose size is limited by material and dimensions which can sustain large temperature differentials, there is no lower limit to the extent in which FCs can be miniaturized. Just as the appearance of microchips first improved existing technologies and then gave rise to completely new technologies that couldn't even have been imagined at that time, FCs will also at first improve existing services but may at a later stage restructure the way the world thinks about energy. In a comparison of FCs with batteries and ICEs it can be said that, like an ICE, a FC's fuel is stored external to it in a separate tank whereas a battery's fuel is stored inside the battery. However, unlike an ICE, which generates energy in the form of a rotating shaft, a FC generates electrical energy very similar to a battery (Scott 2004:1089-1090).

The discussion that follows consists of two parts. The first explains the operation of a fuel cell stack together with its various components. This is then followed by a discussion regarding the

At the anode of each cell, H_2 is oxidized, with the aid of the platinum (Pt) catalyst according to the equation :

$$2H_2 \rightarrow 4H^+ + 4e^- \qquad (2.1)$$

The membrane of the FC is a very good conductor of protons, while also serving as an insulator regarding electron flow. The H^+ ions can thus move freely through the membrane to the cathode side where they recombine with the electrons, coming from the external electric circuit or bipolar plate, together with oxygen to form water. The reduction reaction at the cathode is given by :

$$O_2 + 4H^+ + 4e^- \rightarrow 2H_2O \qquad (2.2)$$

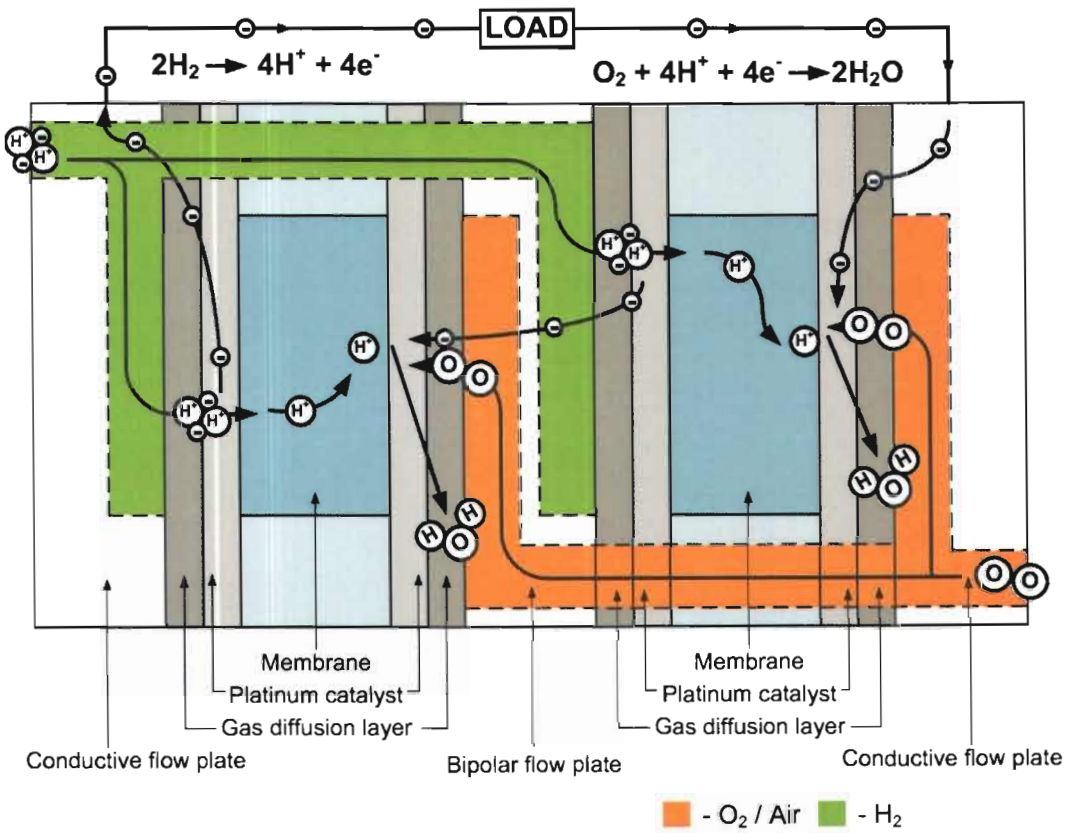

Figure 1 Operation of a FC stack

The only byproducts of a FC are water and heat generated by the chemical reaction. The overall reaction of a FC using H_2 and O_2 can be given by :

$$2H_2+O_2 \rightarrow 2H_2O \quad (2.3)$$

which is also equivalent to the more simple form :

$$H_2+\frac{1}{2}O_2 \rightarrow H_2O \quad (2.4)$$

Even if the FC is not connected to an external load and there are not electrons flowing from the anode to cathode, there is still a flow of protons in the membrane, but in both directions, so that no nett current is generated (Scott 2004b:1206).

To determine the theoretical output voltage of a FC, the chemical energy of H_2, O_2 and H_2O must be considered. The most important factor regarding the chemical energy of the H_2, O_2 and H_2O is the Gibbs free energy. Gibbs free energy can be defined as the energy available to do external work, neglecting any work done by changes in pressure or volume (Larmine & Dicks 2003:28). In a FC, the external work involves moving electrons through the electric circuit connected to the cell. Furthermore, when defining the point of zero energy as pure elements in their normal state at standard pressure and temperature (25 °C and 100 kPa), the term 'Gibbs free energy of formation' is used, indicated by the symbol G_f. In a FC, the change of Gibbs free energy of formation (ΔG_f) must be used to determine the energy released and is given by the equation :

$$\Delta G_f = G_f \text{ of products - } G_f \text{ of reactants} \quad (2.5)$$

or, when considering quantities in 'per mole' :

$$\Delta \overline{g_f} = \overline{g_f} \text{ of products - } \overline{g_f} \text{ of reactants.} \quad (2.6)$$

If equation (2.6) is applied to the overall FC reaction given by equation (2.4), $\Delta \overline{g_f}$ for a FC can be calculated by

$$\Delta \overline{g_f} = \left(\overline{g_f}\right)_{H_2O} - \left(\overline{g_f}\right)_{H_2} - \frac{1}{2}\left(\overline{g_f}\right)_{O_2} \quad (2.7)$$

The Gibbs free energy of formation, given by the above equation, is not constant and changes with temperature and the state of the reactants and products (liquid or gas). The following table gives $\Delta\bar{g}_f$ at different temperatures and conditions (Larmine & Dicks 2003:28-29). The electromotive force (EMF) or open circuit voltage of a hydrogen FC can be calculated with the equation :

$$E = \frac{-\Delta\bar{g}_f}{2F} \text{ V} \tag{2.8}$$

where F is the Faraday constant and is equal to 96 485 C.

Table 1. $\Delta\bar{g}_f$ for the reaction $H_2 + \frac{1}{2}O_2 \rightarrow H_2O$ at various temperatures.

Form of water product	Temperature (°C)	$\Delta\bar{g}_f$ (kJ mol^{-1})
Liquid	25	-237,2
Liquid	80	-228,2
Gas	80	-226,1
Gas	100	-225,2
Gas	200	-220,4
Gas	400	-210,3
Gas	600	-199,6
Gas	800	-188,6
Gas	1000	-177,4

At room temperature, the open circuit voltage of a single FC is :

$$E = \frac{-\Delta\bar{g}_f}{2F}$$
$$= \frac{-\left(-237{,}2x10^3\right)}{2(96485)}$$
$$= 1{,}229\,\text{V}$$

The theoretical open-circuit voltage of two cells connected in series would then be equal to 2,46 V (2 x 1,23 V). The above voltage can also be referred to as the reversible voltage. The term

reversible is used when all the energy in one form is converted to energy in another form (for example, chemical energy into electrical energy) without any energy being converted into another form, for example heat. The process just described would then be called a reversible process. An irreversible process would be one where one form of energy (chemical) is converted into another form (electrical) together with other forms of energy like heat. The energy converted into heat can then be seen as an energy loss and is also called an irreversibility, since this energy cannot be converted back into the original form. There are a number of these irreversibilities, or losses, present in a fuel cell which all contribute to the practical voltage of the FC being lower as the one calculated above. All these losses and their effects are discussed in a later section.

From table 1, it can be seen that $\Delta\bar{g}_f$ decreases with increasing temperature. This means that an increase in temperature would lead to a decrease in cell voltage. However, the voltage losses in a FC are nearly always less at higher temperatures, resulting in higher cell voltages at higher temperatures (Larmine & Dicks 2003:33).

2.3 PEMFC components

One of the biggest challenges currently facing FC technology is the cost of the materials used to make the various components of a FC (Murphy *et al.* 2003:3829). In order to enable the large scale commercialization of fuel cells, materials must be selected that are easy to manufacture at low cost, but still meet the various requirements of the particular component. The following components of a FC will be discussed with reference to the function that they perform in a FC and the different materials that can be used to manufacture these components from :

- Gas diffusion layer (GDL).
- Membrane electrode assembly (MEA).
- Bipolar plate (BP).
- Gaskets for sealing.

2.3.1 Gas diffusion layer (GDL)

A GDL is used to ensure the distribution of reactant gasses over the entire membrane surface area. It also serves as an electrical connection between the catalyst layer on the membrane and the bipolar plates. A GDL also protects the thin catalyst layer and helps with excess product

water removal away from the membrane (Larmine and Dicks 2003:73). The sketch in figure 2 explains the purpose of a GDL (Inoue *et al.* 2005:3).

Materials used in the manufacturing of GDL should have good electrical conductivity, resistance to corrosion and should be porous to allow reactant gas flows as well as the flow of product water. Altering the composition of the GDL, as well as its thickness, can dramatically influence the performance of a FC.

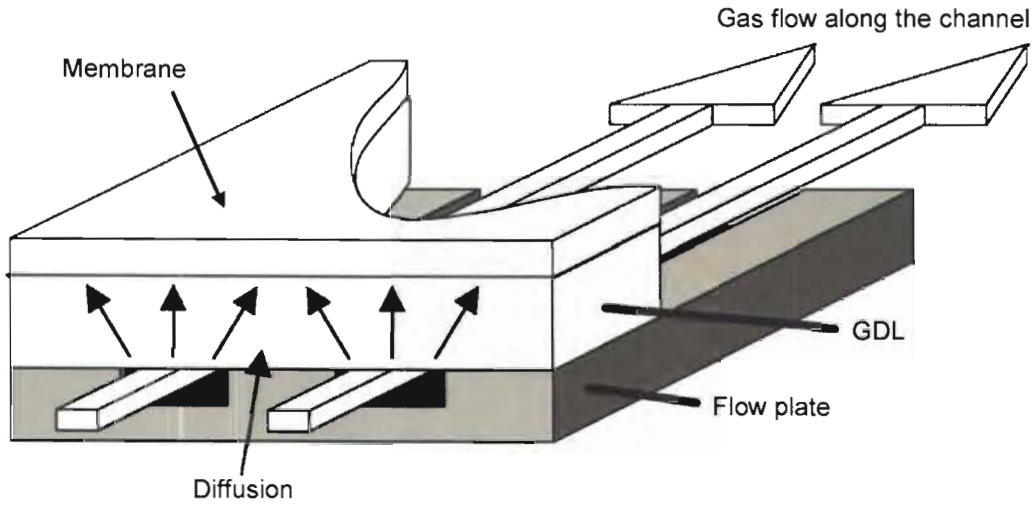

Figure 2 Purpose of a GDL (Inoue *et al.* 2005:3)

The GDL is treated with PTFE in order to make it hydrophobic which prevents water saturation of the GDL. Excess water will thus be pushed out of the GDL (Park *et al.* 2004:183). According to Prasanna *et al.* (2004:154), a PTFE content of 20 percent will result in the best FC performance. Although the PTFE content can affect FC performance since increasing PTFE content can lead to a decrease in GDL porosity, the thickness of the GDL has a much greater effect on cell performance. As the thickness of the GDL increases, its electrical resistance becomes less, resulting in reduced ohmic polarization. However, a thicker GDL can lead to flooding problems and a longer diffusion path length (Jordan *et al.* 2000:250).

GDLs that are manufactured from carbon paper tend to be brittle while carbon cloth GDLs are more flexible. GDLs made from carbon cloth are thicker and can absorb more water. They also tend to fill small gaps and other irregularities in BPs and so simplify mechanical assembly. Since carbon cloth GDLs are more flexible, they will slightly expand into the flow channels and can

hinder the flow of reactants through these channels (Larmine and Dicks 2003:74). A GDL that is too thick can lead to a decrease in cell performance since the oxygen path is then too long. A GDL that is too thin, on the other hand, can lead to an increase in contact resistance between the GDL and catalyst layer on the membrane and also result in a decrease in cell performance (Chu *et al.* 2003:1). According to Vengatesan *et al.* (2005), a thin GDL improves the gas supply and helps with the removal of product water but it has poor mechanical properties and high electrical resistance.

The porosity of the GDL also plays a role in the performance of PEMFCs where a FC in which GDLs with larger porosity are used will consume greater amount of oxygen so that a higher current density is created and a better FC performance is obtained (Chu *et al.* 2003:1). However, the contrary may be true when using very thin membranes because an in increase in cell performance with GDLs with low porosity has been observed by Vengatesan *et al.* (2005). As the amount of product water present in the GDL increases, its effective porosity will become lower and the performance of the cell will deteriorate. At higher current densities, where the output voltage depends mostly on the mass transfer rate of the reactants, the porosity of the GDL has a greater effect than at lower current densities (Chu *et al.* 2003:1).

2.3.2 Membrane electrode assembly (MEA)

The most widely used material in the manufacturing of MEAs is Nafion, a sulphonated fluoro-polymer. The base material is a polymer called polyethelyne which is then modified by substituting fluorine for the hydrogen, creating polytetrafluoroethelyne (or PTFE). The final stage in making the electrolyte membrane is by sulphonating the PTFE by adding a side chain ending in sulphonic acid (HSO_3) to the PTFE molecule (Larmine and Dicks 2003:69-71). Figure 3 shows the structure of the membrane molecule (Larmine and Dicks 2003:70). The PTFE molecule is highly hydrophobic and repels product water from the membrane. The sulphonic acid side chain, on the other hand, is highly hydrophilic and attracts water. This means that Nafion consists of hydrophilic regions within an overall hydrophobic material. The hydrophilic regions can absorb large quantities of water which leads to hydrated regions in the membrane. Within these hydrated regions, H^+ ions are weakly attracted to the SO_3^- group and are able to move freely (Larmine and Dicks 2003:70). This process enables the membrane to serve as a proton conductor. The main features of Nafion are summarized by Larmine and Dicks (2003:71) as :

- High chemical resistance.
- High mechanical strength which allows for thin films to be created.

- Nafion is acidic.
- Able to absorb large quantitities of water.
- When sufficiently hydrated, H^+ ions can move freely through the material.

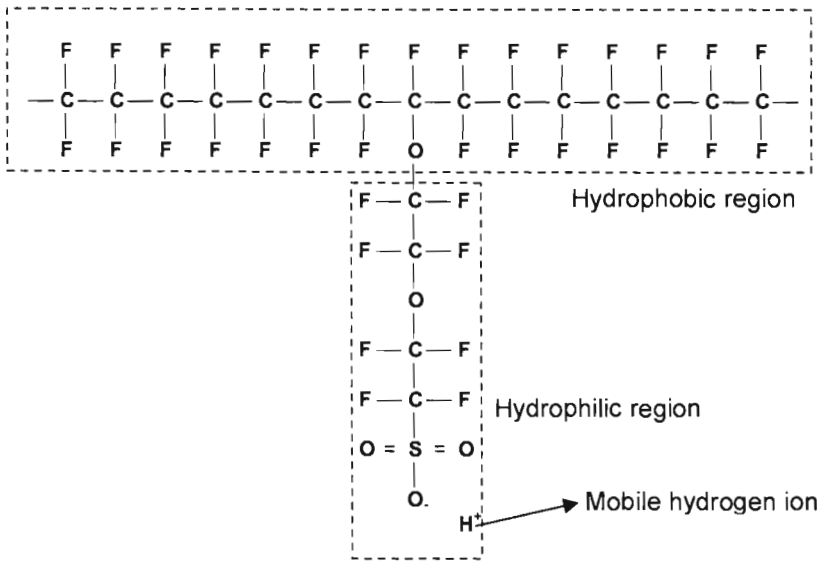

Figure 3 The chemical structure of Nafion (Larmine and Dicks 2003:70)

Since the membrane must be hydrated in order to be proton conductive, the reactants must be humidified before entering the cell. It is possible to operate a FC under dry conditions with the product water from the electrochemical reaction being the only source of hydration. This can offer significant cost savings, but effective water management within the cells becomes crucial for satisfactory FC performance when no external humidification is used (Vengatesan *et al.* 2005:1).

Depending on the amount of water present in the membrane, the flow of protons is associated with a drag of water molecules from the anode to the cathode. This process is called electro-osmotic drag and creates, together with the electrochemical water production, an accumulation of water at the cathode side. The higher water concentration between the anode and the cathode causes back diffusion, which works against the drying out of the membrane from the anode side. The magnitude of this concentration gradient is influenced by the thickness of the membrane, the amount of water present in the membrane and the humidity of the reactant gases. Thinner membranes enhance the back diffusion of water from cathode to anode and allow operation of the PEMFC under dry conditions. The back-diffusion of water from the

cathode to the anode is the dominant process for water management in the cell over a wide range of operating conditions. Water produced by the electrochemical reaction can be sufficient to keep the anode in a humidified state at temperatures up to 70 °C at ambient pressure. Self-humidifying proton conducting membranes with added inorganic materials are also currently being used in PEMFCs. These membranes are able to retain water even at higher temperatures and thus improve cell performance under dry conditions. By adding these inorganic particles, however, the resistance of the membrane is increased. Another problem with self-humidifying membranes is the tedious process involved in their manufacturing (Vengatesan *et al.* 2005:2).

It was stated above that the thickness of the membrane has an influence on the performance of a FC. Chu *et al.* (1999:227) reported that the current density of a FC was significantly enhanced by decreasing the membrane thickness from Nafion 117 (175 μm) to Nafion 112 (50 μm). Vengatesan *et al.* (2005:2) have found that further decreasing the membrane thickness from 50 μm (Nafion 112) to 25 μm, resulted in a significant increase in cell performance under non-humidified conditions at normal operating temperatures (35 – 70 °C). When a membrane is too thin, higher temperatures causes severe water loss due to evaporation.

2.3.3 Bipolar plate (BP)

Bipolar plates are crucial components of a PEMFC and make up a significant part of the volume, weight and cost of a PEMFC stack. They are used, together with GDLs, to distribute fuel and oxidant uniformly over the entire membrane surface area. They also serve as an electrical connection between adjacent cells, remove heat from the active area and prevent leakage of gasses between the anode of one cell and the cathode of the next. In a typical PEMFC stack, bipolar plates account for about 80 percent of the weight and 45 percent of the cost of the stack. Because of this, the BPs must be made from inexpensive and lightweight materials while at the same time minimizing the manufacturing costs. The most widely used materials for the manufacturing of BPs include graphite, coated and uncoated metals and graphite polymer composites. Materials used for the manufacturing of BPs should have the following properties (Hermann *et al.* 2005:1297) :

- High electrical conductivity.
- Thermal conductivity should be as high as possible.
- High permeability to reactant gas flows.

- High corrosion resistance.
- Low density.
- High compressive strength.

Flow channels (also called flow fields) are machined, stamped or moulded (depending on the BP material) into the surface of both sides of a BP. These channels are used to distribute the reactant gases evenly over the entire membrane surface area as well as serving as a path through which excess product water can exit the cell. Figure 4 shows different flow channel designs most commonly used in PEMFCs.

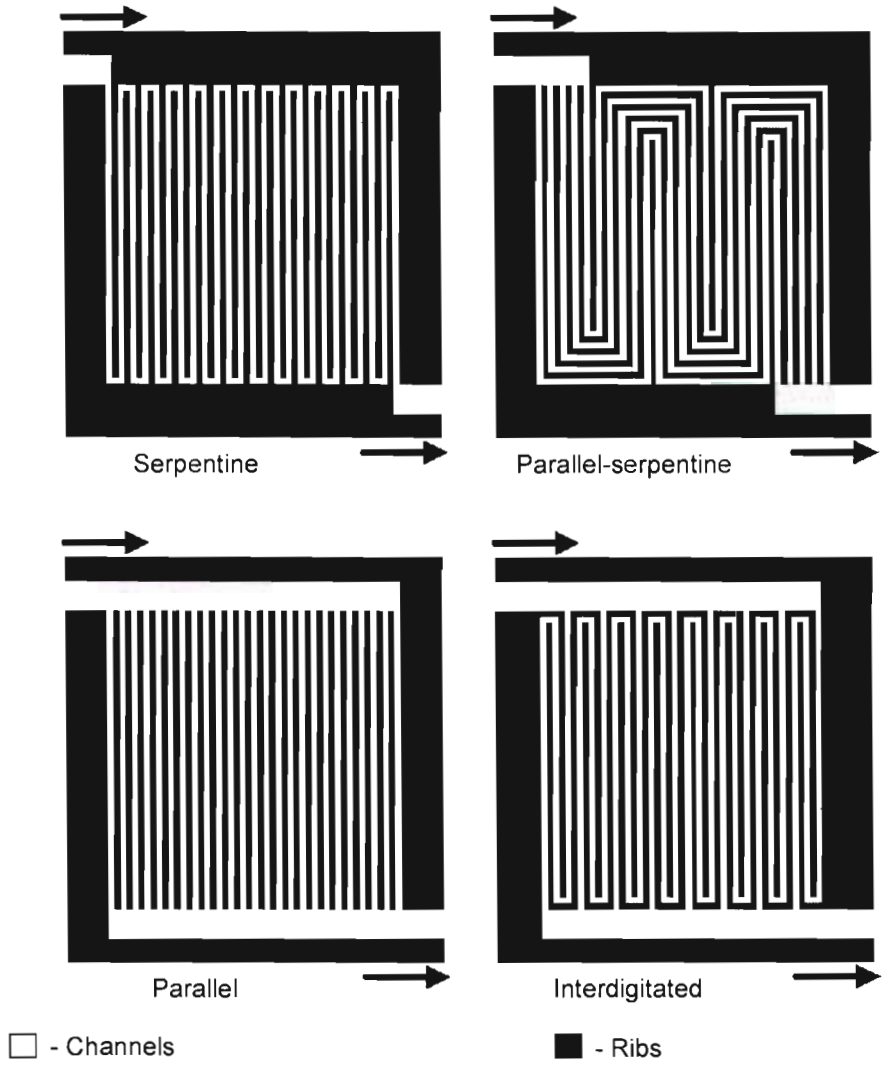

Figure 4 Different flow field designs (Inoue *et al* 2005:12)

A serpentine flow field is created by forming a continuous channel in the surface of the BP. FCs containing serpentine flow fields have to be operated at a higher pressure to ensure that water blocking the channels is pushed out of the cell. To prevent channel blockages, parallel or parallel-serpentine flow channels can be used. When a blockage occurs in one channel, gas will still be allowed to flow through the other channels. Interdigitated flow fields can aid with water management within the cell since the reactant gases are forced over the rib of the BP and into the GDL, pushing water with it. To do this, a higher pressure is needed to ensure a continuous flow through the cell.

Smaller channel and rib areas are needed to achieve higher current densities. Increasing the shoulder areas requires the use of a GDL with higher porosity to allow the distribution of the reactant over the entire membrane surface area (Guvelioglu and Stenger 2005). An optimum width of between 0,7 mm and 1 mm for both the channels and ribs was found by Scholta *et al* (2005:1). As the channel widths becomes smaller, manufacturing efforts increase as well the probability of product water blocking the channels. When operating a FC at higher current densities, smaller channel and rib widths are better (Scholta *et al* 2005:1). This has also been confirmed by experiments done by Yoon *et al* (2005:1363). The depth of the channel is also important, as shown by Inoue *et al.* (2005:14) and at higher current densities the cell output voltage will be higher when the channel is shallow (about 0.5 mm).

Graphite has been the most widely used material for BPs because of its resistance to corrosion in the PEMFC environment and low electrical resistance. Low mechanical strength and high cost of graphite have created the need to find better materials. Machining the flow channels into the graphite BPs also requires a long time on expensive machines (Hermann *et al.* 2005:1298-1299). Since graphite is inherently porous, either thicker BPs must be used to prevent leakages adding to the stack's volume or weight, or the graphite must be impregnated with a resin in order to make it impermeable. This further adds to the cost of graphite BPs (Larmine and Dicks 2003:97).

Other materials that have potential for use in BP manufacturing are metal which have good electrical and thermal conductivity as well as mechanical stability. The fact that metals are impermeable to reactant gas flows makes it possible for thinner plates to be used which allows for the flow channels to be formed by stamping. Since BPs are exposed to temperatures of about 80 °C and a pH of 2-3, metals are prone to corrosion and dissolution. Dissolution leads to mobile metal ions which can poison the membrane causing a drastic decrease in cell

performance. The output of the cell can be further decreased with the forming of a corrosion layer on the surface of the BP. To avoid corrosion, a conductive coating can be applied to metallic BPs. The coating should adhere to the base metal without exposing it (Hermann *et al.* 2005:1300). Wind *et al.* (2002:256) have reported that the performance of FCs using coated stainless steel BPs is the same as in cells using graphite BPs. Some metals resist corrosion by forming a surficial oxide film. This results in an increase in plate resistance and must be prevented by coating the metal with a protective layer (Murphy *et al.* 1998:3832).

Metal or carbon-based composites offer an attractive alternative to both graphite and metal BPs. Composites can be moulded into any shape and are very lightweight material but the electrical conductivity of composite BPs is lower than that of metals and graphite (Hermann *et al.* 2005:1301). It has been estimated that by using composites or metal alloys, the cost of BPs would only be 15-29 percent of the total stack cost (Cho *et al.* 2004:178). Experiments were performed in which BPs made from carbon-based composites were compared with graphite BPs. The composite BPs were composed of 90 percent graphite powder, mixed with 10 percent unsaturated polymer and a small amount of organic solvents and additives. BPs can be manufactured using this material by either hot-pressing it into plates and then machining the flow channels, or by moulding the compound powder directly into the final BP by applying compression pressure at a certain temperature. These plates were reported to perform in a very similar manner to that of graphite BPs (Cho *et al.* 2004:178).

Since metal is non-permeable to reactant gas flow, it is possible to manufacture BPs using a combination of thin metal sheets, supported by a lightweight, non-conductive, material (Murphy *et al.* 1998:3830). A material that fits the above description very well is printed circuit board (PCB), which consists of a thin copper layer (about 35 μm) on top of a thicker fiberglass substrate (about 1,6 mm). O'Hayre *et al.* (2003:459) demonstrated the use of PCB BPs to produce FC stacks delivering a power output of over 200 W. Some of the advantages in using PCB for the manufacturing of BPs are (O'Hayre *et al.* 2003:459) :

- Established technology.
- Fast prototyping times.
- Cost efficient prototyping.
- High design flexibility.
- Lightweight.

PCB technology has been used in the electronics industry for many year and well established tools and methods regarding PCB manufacturing currently exist. This allows for complex BP designs to be produced using low-cost methods in a fraction of the time needed for other materials. Although copper has a very low electrical resistance with a specific resistivity of 16,73 $\mu\Omega$.mm, the use of copper in a FC environment leads to the formation of mobile oxidized copper species which can travel to the membrane (Murphy *et al* 1998:3830). This will drastically decrease the proton conductivity of the membrane, resulting in a decrease in cell performance. In order to avoid corrosion of the copper and ensure the durability of copper BPs, the copper must be coated with a protective layer. According to Schmitz *et al.* (2004:197), the use of electroplated nickel (Ni) and chrome (Cr) can lead to long-term FC operation using PCB BPs and can increase the lifetime of a FC from less than 100 hours (only copper) to over 1000 hours (copper coated with Ni and Cr). Some metals, including nickel and titanium, resist corrosion through the formation of an oxide film on their surfaces which prevents the oxidation of the metal underneath the oxide film (Murphy *et al.* 1998:3832). This oxide film has a high resistance though, and its formation can be prevented by coating the base metal with a protective layer of gold or chrome.

2.3.4 Gaskets

Proper sealing of a PEMFC stack is very important in order to separate the oxygen and hydrogen gas from each other and to prevent any reactant gas leakages out of the stack. A typical sealing material is silicone. A mixture of hydrogen and oxygen of a certain ratio can explode. In a FC, however, it is unlikely for an explosion to occur since the platinum catalyst stimulates the reaction of hydrogen and oxygen. The heat of this catalytic combustion creates hot spots in the membrane though and can ultimately destroy it. After extensive degradation of the membrane, more hydrogen and oxygen will mix, usually resulting in an open fire (Schulze *et al.* 2004:223).

2.4 Mathematical model of a PEMFC

It was stated earlier that practical FC voltages are lower than the theoretical open-circuit voltage of 1,23 V and that the voltage of the cell becomes less as more current is drawn from it. Even the practical open-circuit voltage can never reach the theoretical value. A typical open-circuit voltage for a FC is around 0,9 V. The next section will discuss the various factors that contribute to the voltage-current characteristics of a FC. Figure 5 shows how the output voltage of a single

The voltage-current curve shown above can also be referred to as a polarization curve since the losses or sources of voltage drop can also be called activation polarization, ohmic polarization and concentration polarization. The operating point of the FC should always be kept in the ohmic polarization region to ensure safe operation of the cell and to maximize the efficiency of any power converter systems connected to the cell (Choi *et al.* 2005:246).

- Activation losses are caused by a portion of the cell voltage being lost in keeping the chemical reaction going that transfers electrons between the electrodes. This voltage drop has a very non-linear form and contributes, in part, to the first region of the graph in figure 5. Activation losses can be described by the Tafel equation :

$$\Delta V_{act} = A\ln\left(\frac{i}{i_0}\right) \quad \text{V} \tag{2.9}$$

In the equation above, i is the fuel cell current density and i_0 is the current density where the voltage drop begins to move away from zero. For example, if i_0 is 100 mA.cm^{-2}, there will be no voltage drop until the current density i is greater than 100 mA.cm^{-2}. The Tafel equation only holds true when $i > i_0$. A is a constant and is given by

$$A = \frac{RT}{2\alpha F} \tag{2.10}$$

where T is the temperature, F is the Faraday constant and R is the universal gas constant. The constant α is called the charge transfer coefficient and refers to the part of the electrical energy that is used in changing the rate of the electrochemical reaction. The value of A is always in the range of 0 to 1 and depends also, apart from the type of reaction, on the material that the electrodes are made of. Note that equation (2.9) can also be written as

$$\Delta V_{act} = A\ln(i) - A\ln(i_0) \text{ V} \tag{2.11}$$

Activation overvoltage is the most important cause of voltage drop in low- and medium-temperature fuel cells and occurs mainly at the cathode in cells using hydrogen as fuel. At higher temperatures and pressures, activation overvoltage becomes less important (Larmine and Dicks 2003:48-53). Another way of explaining activation losses is with the fact that electrochemical

reactions proceed rather slowly. This makes it necessary for the reactions to be activated by using an increased voltage drop to pull the charge particles across electrode-electrolyte interface. After this voltage drop, the current begins to flow more rapidly (Scott 2004b:1209).

- Another cause of voltage drop in a FC is from fuel crossover and internal currents. Although the electrolyte membrane in a FC is designed to be impermeable to reactant gas flow and to be only proton conductive, it is still possible for a small amount of reactants to permeate through the membrane from one side of the cell to the other. This, together with a small amount of electron flow though the membrane, causes a significant voltage drop in the open circuit voltage of low-temperature FCs. If a total internal current density i_n is caused to flow through the cell by fuel crossover and internal currents, this voltage drop can be combined with the activation loss :

$$\Delta V_{act} = A \ln\left(\frac{i + i_n}{i_0}\right) \text{ V} \tag{2.12}$$

Typical values for the above equation in the case of a low-temperature FC is A = 0,06 V, i_0 = 0,04 mA.cm^{-2} and i_n = 3 mA.cm^{-2} (Larmine and Dicks 2003:53-56).

- The second region of the graph in figure 5 is fairly linear and is caused by the electrical resistance of the electrodes as well as the resistance to proton flow through the membrane. This voltage drop is proportional to the current and can be modeled by :

$$V = IR \text{ V} \tag{2.13}$$

Since the previous two losses were modeled using current density, the total ohmic resistance in the above equation must be converted to an area specific resistance. If the current density is given in terms of mA.cm^{-2}, then the area specific resistance must be in terms of kΩ.cm^2. The equation for ohmic losses then becomes :

$$\Delta V_{ohm} = ir \text{ V} \tag{2.14}$$

The internal resistance of a FC can be reduced by using electrodes with a very low resistance and by making the membrane as thin as possible. Making the membrane too thin, however, can be impractical since the membrane still have to be mechanically rigid (Larmine and Dicks 2003:56-57).

- The final cause of voltage drop in a FC is shown in region 3 of the graph in figure 5. This loss is referred to mass transportation loss or concentration losses. When the oxygen needed by the cell is supplied in the form of air, there will be a reduction of the concentration of oxygen in the air around the electrodes as the oxygen is used by the cell. On the anode side, where hydrogen is used, there will also be a reduction of hydrogen pressure as more hydrogen is consumed as a result of higher currents being drawn from the cell. This reduction in pressure at both the anode and cathode will result in a voltage drop :

$$\Delta V = \frac{RT}{2F} \ln\left(\frac{P_2}{P_1}\right) \text{ V} \tag{2.15}$$

if the pressure is reduced from P_1 to P_2. The problem with the above equation is that the voltage drop is in terms of pressure and not current or current density. This equation can be converted so that it is in terms current density as shown in Larmine and Dicks (2003:58). The resulting equation, however, tends to be inaccurate under practical conditions and is not suitable for accurately modeling practical FC behavior. However, an alternative model does exist in which the concentration losses are given by

$$\Delta V_{trans} = me^{ni} \text{ V} \tag{2.16}$$

where m and n are constants (Larmine and Dicks 2003:59). This equation fits very well with experimental data if m and n are chosen correctly. Typical values for m and n are 3×10^{-5} V and 0,008 $cm^2.mA^{-1}$ respectively.

The above losses can be combined and subtracted from the theoretical open circuit voltage E, to give the actual FC output voltage over its entire current range :

$$V = E - \Delta V_{ohm} - \Delta V_{act} - \Delta V_{trans} \text{ V} \tag{2.17}$$

$$V = E - ir - A\ln\left(\frac{i + i_n}{i_0}\right) - me^{ni} \text{ V} \tag{2.18}$$

Since the crossover current i_n is very small and only useful for explaining the initial drop in voltage, it can be omitted. The above equation can then be simplified to

$$V = E + A\ln(i_0) - ir - A\ln(i) - me^{ni} \text{ V} \tag{2.19}$$

The first two terms in this equation are constant, regardless of the current drawn from the cell, and can be replaced with a practical open circuit voltage, E_{OC} :

$$V = E_{OC} - ir - A\ln(i) - me^{ni} \text{ V} \tag{2.20}$$

This equation has been reported to give an excellent fit with experimental FC data (Larmine and Dicks 2003:60). In the case of a FC stack, comprised of N_C identical cells, equation (2.20) can be rewritten as (Jiang and Chu 1999:132) :

$$V_{STACK} = N_C E_{OC} - N_C ir - N_C A\ln(i) - N_C me^{ni} \text{ V} \tag{2.21}$$

The constants in the above equation can be determined from analysis of experimental data from small FC stacks of only a few cells. The value of N_C can then be adjusted in order to predict the behavior of a 100 W FC stack. The resulting equation will then be used to design an equivalent electronic circuit model of a 100 W FC stack to enable the simulation of the stack together with other electronic circuitry that will make up the complete UPS system.

2.5 Electronic circuit model of a PEMFC

Most of the models that have been developed for FCs are based on complex chemical phenomena or are very mathematical in nature. This makes it impossible for these models to be used to simulate the FC together with power converters or any other electronic subsystems. Yu and Yuvarajan (2005:238) developed a novel circuit model for a PEMFC which includes all the important characteristics of a FC stack. The model is based on the non-linearity of a diode and the current control feature of bipolar junction transistors (BJT). The diode is used to model the ohmic losses and activation losses, while the two BJTs are used to model concentration losses. This circuit model can be used in an electronic simulation package to simulate the behavior of a FC stack together with any other electronic circuitry.

In the circuit diagram in figure 6, E is the theoretical open circuit voltage of the FC stack and RL is the load connected to it. The voltage across the load resistor is V_{STACK} and can be calculated

using equation (2.21). The capacitor C and inductor L are used to model the dynamic behavior of the FC stack.

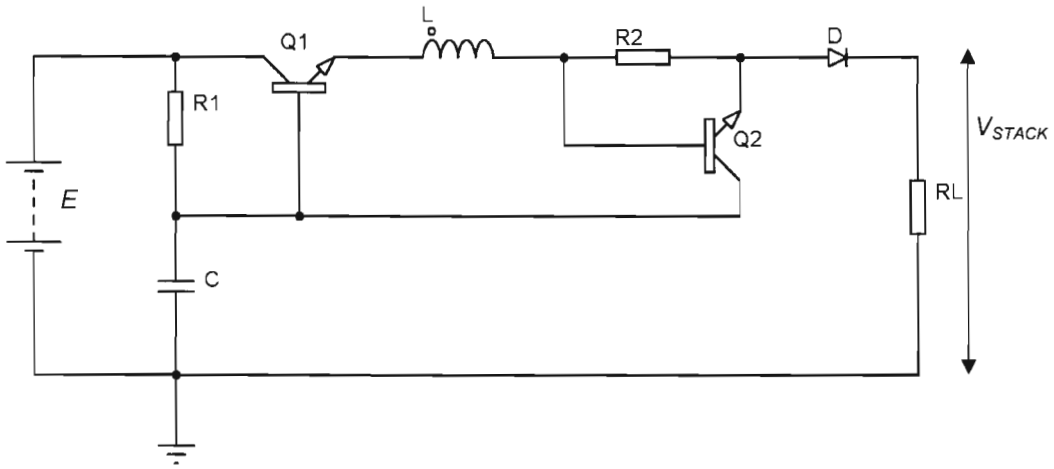

Figure 6 Electronic circuit model of a PEMFC stack (Yu and Yuvarajan 2005:239)

The two transistors, Q1 and Q2, together with R1 and R2 are used to model the concentration losses. The non-linear behavior of the activation losses is represented by the diode D. The ohmic resistance of the diode is also used to model the ohmic losses of the FC stack.

The relationship between the voltage across a diode (V_D) and the current through it (I_D) is given by the equation

$$V_D = nV_T \ln\left(\frac{I_D}{I_{SD}}\right) \text{ V, where } V_T = \frac{kT}{q} \text{ V} \qquad (2.22)$$

where n is the emission coefficient, I_{SD} is the saturation current and V_T is the thermal voltage in terms of the Boltzmann's constant (k), absolute temperature (T) and electronic charge, q. This equation exactly resembles equation (2.9) for the activation losses in a FC (Yu and Yuvarajan 2005:240).

The transistors, Q1 and Q2, together with R1 and R2 form a current limiting circuit used to model the concentration losses of the FC stack. R2 acts as a current sensing resistor so that when the current through it exceeds a certain limit, Q2 will start conducting, reducing the base voltage of Q1. This will cause the emitter voltage of Q1 to decrease at an exponential rate. The two

transistors are assumed to be identical with current gain β and base-emitter voltage V_{BE}. The variation of the output voltage (V_{STACK}) as a function of load current (I_O) can be determined using the circuit in figure 7 (Yu and Yuvarajan 2005:240).

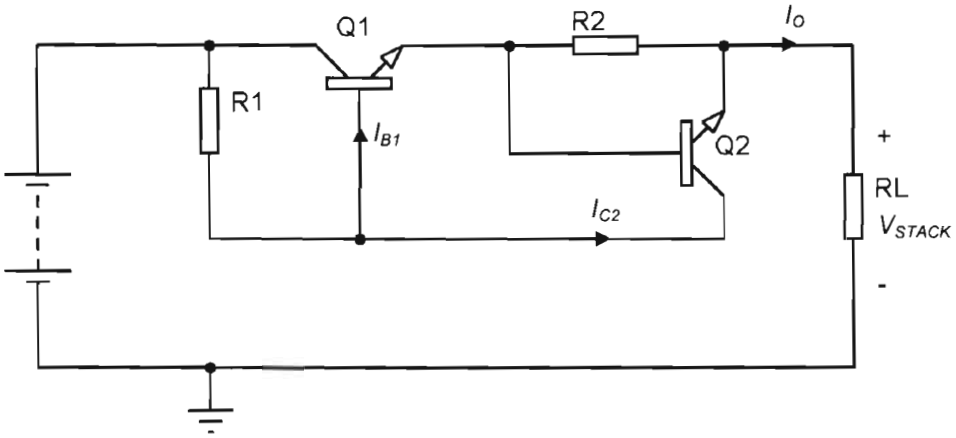

Figure 7. Modeling the concentration losses of a FC stack.

The base current of Q1 and the collector current of Q2 can be written as :

$$I_{B1} = \frac{I_O - I_{C2}}{1+\beta} \text{ A} \tag{2.23}$$

$$I_{C2} \approx I_S e^{\frac{I_O R2}{V_T}} \text{ A} \tag{2.24}$$

where I_S is the saturation current of Q1 and Q2 and V_T is the thermal voltage of the transistors as given in equation 2.22. The output voltage can then be written as :

$$V_O = V_S - \text{R1}(I_{B1} + I_{C2}) - V_{BE1} - \text{R2}(I_O - I_{C2} - I_{B2}) \text{ V} \tag{2.25}$$

By substituting equations (2.23) and (2.24) into equation (2.25) and assuming that β is large, the output voltage can be simplified to :

$$V_O = V_S - \text{R2} \cdot I_O - \text{R1} \cdot I_S e^{\frac{\text{R2} \cdot I_O}{V_T}} - V_{BE1} \text{ V} \tag{2.26}$$

Combining equations (2.22) and (2.26), the total FC output voltage can be written as :

$$V_O = V_S - V_{BE1} - I_O R2 - nV_T \ln\left(\frac{I_O}{I_{SD}}\right) - R1 \cdot I_S e^{\frac{I_O R2}{V_T}} \text{ V} \quad (2.27)$$

It can be seen that this equation is in the same form as equation (2.21). The values of the resistors R1 and R2 determines the shape of the FC's V-I curve in the region where concentration losses becomes dominant (region 3 in figure 5). The value of R2 determines the starting point of the concentration loss region. The rate of change of the voltage in the concentration loss region is determined by the value of R1. The values of R1, R2, n, I_{SD}, I_S and V_{BE} will be determined by comparing equation (2.27) with the one calculated for a 100 W stack using equation (2.21). Typical values of 1 F and 10 mH are used for the values of C and L respectively (Yu and Yuvarajan 2005:240-241).

2.6 Factors influencing PEMFC performance

Not only do various factors influence the performance of FCs, but factors like temperature, pressure and environmental conditions also effects the lifetime of these cells (Knights *et al* 2004:127).

2.6.1 Reactant gas flow rate

When delivering high currents, uneven flow rates together with product water blocking the flow channels can result in starvation conditions in individual cells. In the case of oxygen starvation, protons passing through the membrane will combine with electrons to form hydrogen at the cathode side of the FC which will cause the cell voltage to drop to very low levels or even become negative. When hydrogen starvation occurs at the anode, water will be oxidized to form protons and oxygen. The protons will then pass through the membrane to form water at the cathode side. Recent catalyst technology involves the use of platinum on carbon particles in order to reduce the amount of platinum needed on the anode. When fuel starvation occurs, these types of anodes tend to degrade, resulting in a permanent loss in performance. (Knights *et al* 2004:128). When using air as an oxidant, a higher flowrate is required and product water must be removed at a higher rate to increase the diffusion rate of the oxidant to the catalyst layer (Jordan *et al.* 2000:253). Whadame *et al* (2005:6) noticed that the air flowrate actively

contributed to the removal of product water from the cell and that a higher air flowrate is beneficial in this regard.

2.6.2 Temperature

Operating a FC stack at higher temperatures can be beneficial since less energy has to be spent on the cooling of the stack. Higher temperatures can however lead to a reduction of water content in the membrane, which will cause a decrease in cell performance and shorten the lifetime of the membrane (Knights *et al.* 2004:133).

2.6.3 Pressure

To calculate the theoretical output voltage of a FC at a given temperature and pressure, the Nernst equation can be used (Larmine and Dicks, 2003:36) :

$$E = E_0 + \frac{RT}{2F} \ln\left(\frac{P_{H2} \cdot (P_{O2})^{1/2}}{P_{H_2O}}\right) \text{ V} \qquad (2.28)$$

In the above equation, E_0 is the output voltage at standard temperature and pressure (1,23V). The Nernst equation shows that increasing the temperature and/or pressure will lead to an increase in cell voltage. At higher operating pressures, the electrochemical reaction rate is higher, resulting in higher current densities and more oxygen is consumed at the cathode (Sun *et al.* 2005:133).

2.6.4 Humidity

Water management plays a crucial role in maintaining optimum reliability and durability of FCs. Lack of water in the cell will lead to a reduction in conductivity of the membrane resulting in an increase in ohmic losses. Inadequate water in the membrane can lead to the accelerated degradation of the membrane resulting in holes in the membrane which will cause reactant gas crossover. When fuel crossover occurs, a pressure differential across the membrane can cause one fuel to consume the other, resulting in fuel starvation in the cell. Tests performed by Knights *et al.* (2004:130) have shown that the lifetime of a PEMFC stack was significantly decreased as a result of low humidity conditions. When humidity levels are too high, however, water blockages can occur in the flow channel and GDL, resulting in increased mass transportation losses. This

can be prevented to some extent by increasing the flow rate of the reactant gases to ensure that the water is pushed out by the reactant gases or to increase the porosity of the GDL (Knights *et al.* 2004:129-132).

The humidity of the reactant at the anode (hydrogen) has a greater effect on cell performance than the humidity of the air entering the cathode. Back diffusion of water from the cathode to the anode is not sufficient to keep the membrane hydrated at higher currents (Guvelioglu and Stenger 2005). It is possible, under optimized conditions, to only humidify the incoming air and not the hydrogen as shown by Whadame *et al* (2005:2). At high cell currents, water management becomes crucial in maintaining a balance between good gas diffusion and ionic conductivity in the membrane. Although increased water content in the membrane can lead to better proton conductivity, excess water can be condensed into liquid phase in the GDL. This can hinder gas diffusion, resulting in increased concentration losses (Park *et al* 2004:182). Williams *et al.* (2004:133) have reported operating a FC stack under dry conditions with reduction of no more than 17 percent of the total stack output power. This leads to a simpler system design since humidifiers are eliminated. However, a larger FC stack is required for the same power output and greater care must be taken in controlling the flow rates of the reactants and the stack temperature.

FC reactants can be humidified using various methods. The simplest involves bubbling the reactants through water. The temperature of the water is controlled, because low water temperature results in less humidity, while higher temperatures will ensure that more water reaches the cell. The product water from the FC can also be recirculated and used for humidification purposes. Other methods involve the direct injection of water vapor or liquid water into the FC. Vapor injection requires a complex cell design, adding to the total stack cost (Wood *et al.* 1998:3797-3798). Direct liquid injection is a mature technology and is widely used on larger FC system where enough energy is available to pressurize the water.

2.7 Secondary storage and DC/DC converter

FCs are low-voltage and high-current devices which makes it necessary for the output voltage of a FC stack to be boosted to a higher, more useful level. For example, when the required output of a FC system is 220 V at 50 Hz, the output voltage of the stack must be boosted to about 400 V_{DC} before it can be converted to the required ac level with a DC-AC inverter (Choi *et al.* 2005:247).

Since it takes a certain amount of time for a FC to reach its maximum power output, a secondary form of electrical storage is necessary. This is especially important in a UPS system where a drop in output voltage cannot be tolerated. There are two main types of electrical energy storage (EES) systems that can be used to supply energy to the UPS load while the FC starts up. These are batteries and ultra capacitors (or supercapacitors). Compared to ultra capacitors, batteries have a high energy storage density and low power density. Batteries also have a limited lifetime and requires significant maintenance. Ultra capacitors have very long cycle lifetimes of over 100 000 cycles, high power densities and high discharge and charge efficiencies (Meacham *et al* 2005:1-2). Using FCs together with supercapacitors in a UPS system have the following advantages (Choi *et al.* 2005:2):

- System is clean, quiet and environmentally friendly.
- The state-of-charge of batteries are not always known, whereas in a FC system the available power is a function of the amount of hydrogen available.
- Due to the fast discharging characteristics of supercapacitors, no delay time is required for the UPS to take over the load.
- Because of the supercapacitor, the system can handle conditions of overload very well.
- As long as reactants gasses are supplied to the cell, continuous power can be delivered.

The low voltage of a FC stack can be efficiently converted to a higher voltage using a simple switch mode boost converter as shown in figure 8. When the switch (S_1) is on, and there is some charge in the capacitor (C_1), an electric current will build up in the inductor (L_1) and the load is supplied by the discharging of the capacitor. The diode (D_1) prevents the discharging of the capacitor through the switch. When the switch is off, the current in the inductor falls, causing the inductor voltage to rise sharply. As soon as the voltage rises above that of the capacitor, the current will flow through the load as well as charge up the capacitor (Larmine and Dicks. 2003:336-337).

If t_{ON} is the time that the switch is on, and t_{OFF} its off-time, then the relationship between the input voltage (V_{IN}) and the output voltage (V_{OUT}) can be described by (Larmine and Dicks 2003:337) :

$$V_{OUT} = \frac{t_{ON} + t_{OFF}}{t_{OFF}} \cdot V_{IN} \text{ V} \tag{2.29}$$

A higher output voltage than that of the input can be achieved by having the switch off for only a short time.

This can be accomplish by varying the duty cycle of a PWM signal. Efficiencies of over 80 percent and up to 90 percent can be achieved using a boost converter (Larmine and Dicks 2003:338). A typical switching device that can be used in a boost converter is a MOSFET.

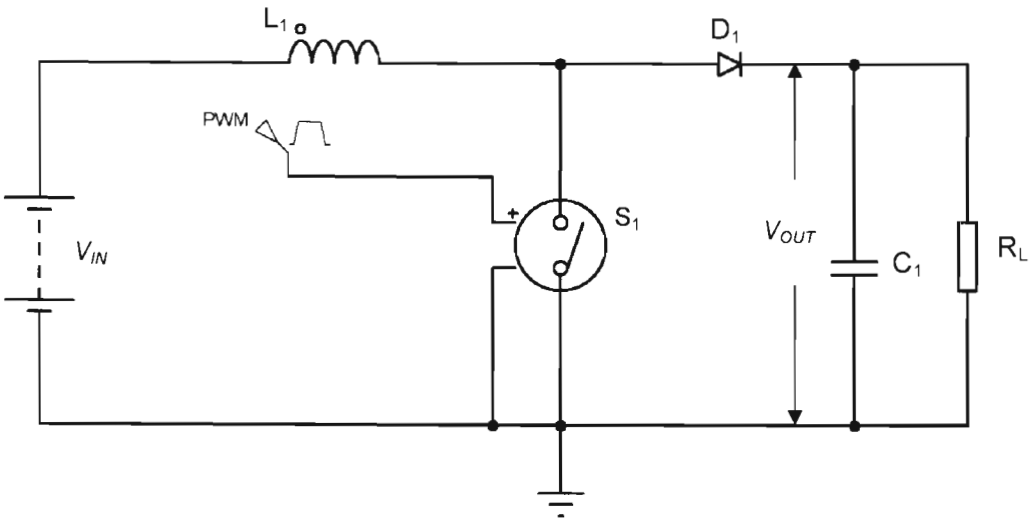

Figure 8 Switch mode boost converter

When the output current of a boost converter increases, the output voltage will decrease. The output voltage will also change as the input voltage changes. It is also known that an increase in output current of a FC will cause the output voltage of the FC to drop. Furthermore, the dc-dc converter can also be used to regulate the output voltage of the supercapacitor whose voltage falls over time as the capacitor discharges. The output voltage of the UPS system, must remain constant however, regardless of all the above mentioned voltage variations. To ensure a constant output voltage, a control system must be implemented that will measure the output voltage (or a portion of it) and adjust the duty cycle of the PWM signal accordingly. The control system can be implemented using a PIC microcontroller, as shown in figure 9, since it has an analog-to-digital converter (ADC) built-in which can be used to measure the output voltage.

The PIC microcontroller is also capable of providing a PWM output signal to switch the MOSFET in the boost converter circuit. Since the input range of the PIC microcontroller's ADC is only 0-5 V, a voltage divider comprising R_1 and R_2, is used to feed only a portion of the higher output voltage back to the controller. A software PID (Proportional Derivative Integral) controller can be implemented on the PIC microcontroller in order to control the duty cycle of the PWM switching signal. PID controllers are extremely robust and are widely used in industry. The PID algorithm is

$$I_k = I_{k-1} + K_I e_k \tag{2.33}$$

Not only is the integral term based on the amount of error but also on how long the error has been present. The final term of equation 2.31, the derivative term, is calculated by subtracting the current error from the previously measured one and multiplying the result with the derivative gain constant, K_D:

$$D_k = K_D\left(e_{k-1} - e_k\right) \tag{2.34}$$

The effect of the derivative term on the output depends on the speed at which the error term changes. A rapid change in the error will result in a bigger contribution of the derivative term on the output (Condit and Butler 2003:6-7). The derivative term is very important in maintaining system stability since it acts as an anticipator. When the error term is decreasing, the derivative term will subtract from the output in an anticipation of an overshoot condition (Charais and Lourens 2004:6).

2.8 Summary

This chapter considered the history of FCs and the theory of operation of a FC stack. The characteristics of a FC's output voltage, both theoretical and practical, were discussed as well as various factors influencing a cell's output voltage and power. Modeling a FC stack using both a mathematical equation and an electronic circuit equivalent was considered. The chapter concluded with a discussion on the use of FCs together with secondary storage devices and power converters in a UPS system. It was seen that there are several advantages in replacing batteries with supercapacitors.

The next chapter discusses the practical, proof-of-concept, design of a low-cost FC stack using PCB technology. The characteristics of this stack is then used to finalize the mathematical model discussed in this chapter. The model is also adapted to describe the characteristics of a 100 W stack. Using the two mathematical models, electronic circuit equivalents are designed for both the small stack and a 100 W stack. The design of a switch mode boost regulator is also described together with the control system needed to maintain a constant output voltage when the converter is connected to a FC stack.

Chapter 3 Design of a PEMFC UPS system

The previous chapter considered the operation of a PEMFC stack together with its characteristics and the various factors that determine its performance. The underlying theory regarding the modeling of a FC stack was also discussed. This chapter focuses on the practical design of a small, low-cost, PEMFC stack. This stack is used to validate both the mathematical model and electronic circuit equivalent of a FC stack. Since these models can be extrapolated to represent a larger stack, as seen in the previous chapter, an electronic circuit model of a 100 W stack is then developed. Finally, the design of a 100 W switch mode boost converter is discussed.

3.1 Design of a low-cost PEMFC stack using PCB technology

This section considers the design of a two-cell, proof-of-concept, FC stack made from low-cost and readily available materials. Flow plates used in the stack were manufactured from copper-clad PCB using standard PCB manufacturing techniques and machines. Each type of cell component is considered in turn, followed by the final stack design.

3.1.2 Bipolar plates

As seen in chapter two, the use of PCB presents several advantages in terms of weight, cost and production time. Standard single-sided FR4 PCB, consisting of 35 μm thick copper layer on a 1,6 mm fiberglass substrate, was used to manufacture the BPs. The BPs were designed using the Eagle software package, normally used to design electronic circuits and PCB layouts. The design was then exported and machined using a PCB milling machine. Figure 10 shows one side of a BP. Two of these plates are placed back-to-back, with a gasket between them, to form one complete BP. An electrical connection must also be made between the copper layers on each BP to conduct electrons form the cathode of one cell to the anode of the next cell.

The width of both the ribs and channels should be between 0,7 mm and 1 mm, as suggested by Scholta *et al.* (2005:1). A width of 1 mm was chosen since this was the smallest width that the milling machine could produce. The depth of the flow channels was chosen as 0,8 mm, about half of the total thickness of the PCB. The dimensions of the BP was 84 mm x 84 mm. This was the smallest size that would still allow adequate sealing of the stack. As can be seen from figure 10, three notches were machined in the BPs to ensure that all plates line up correctly to prevent reactant gas blockages and/or leaks.

Figure 4 in chapter 2 showed different flow field designs. Since the entire PCB BP is not conductive (only the surface is), the use of parallel or parallel-serpentine flow fields will result in isolated sections of copper which would not be able to conduct any current to or from the membrane.

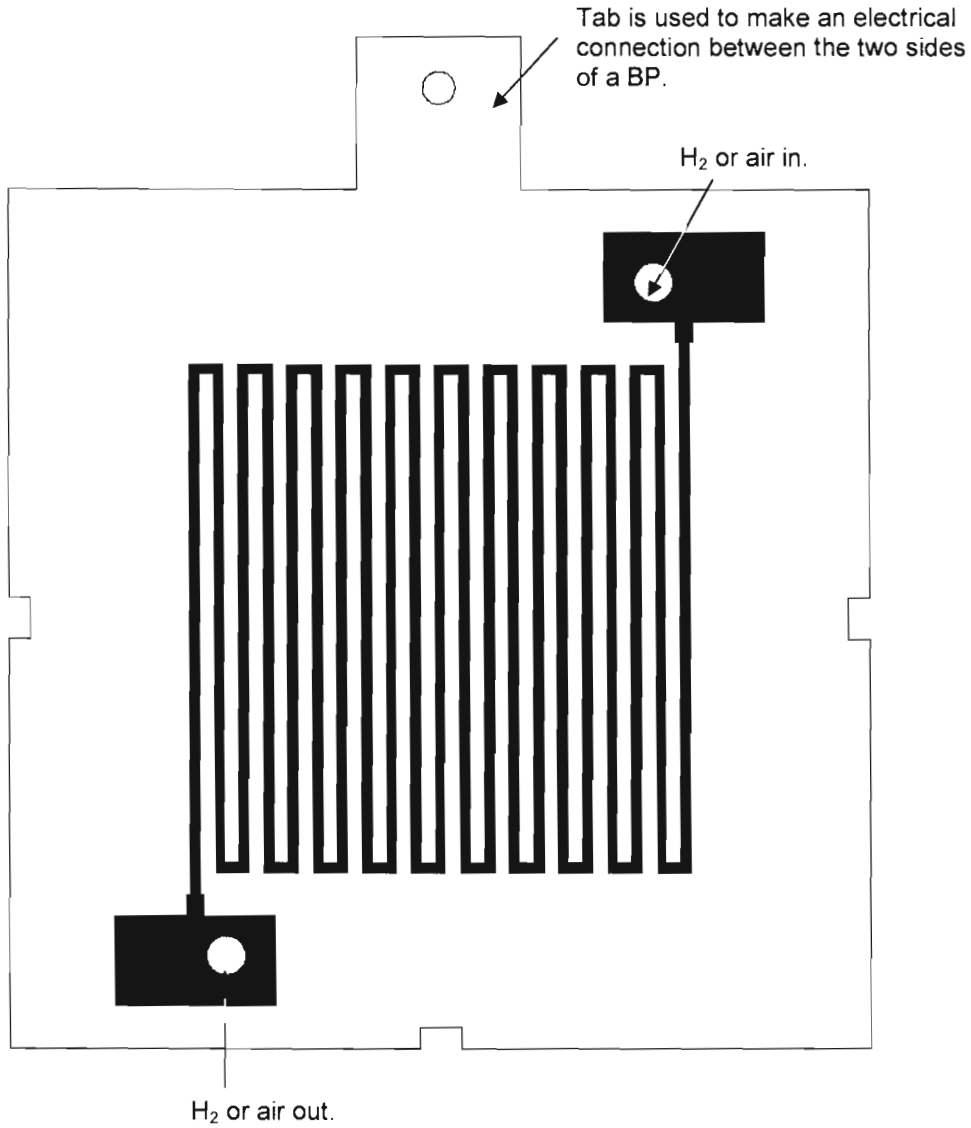

Figure 10 BP plate design

This would also be the case, but to a lesser extent, when using the interdigitated design. In order to protect the copper from corrosion and prevent the poisoning of the membrane, the copper was electroplated with a layer of nickel, followed by a chrome layer. Chrome cannot be plated

directly on copper, hence the need for the nickel layer. Figure 11 shows two chrome plated PCB BPs.

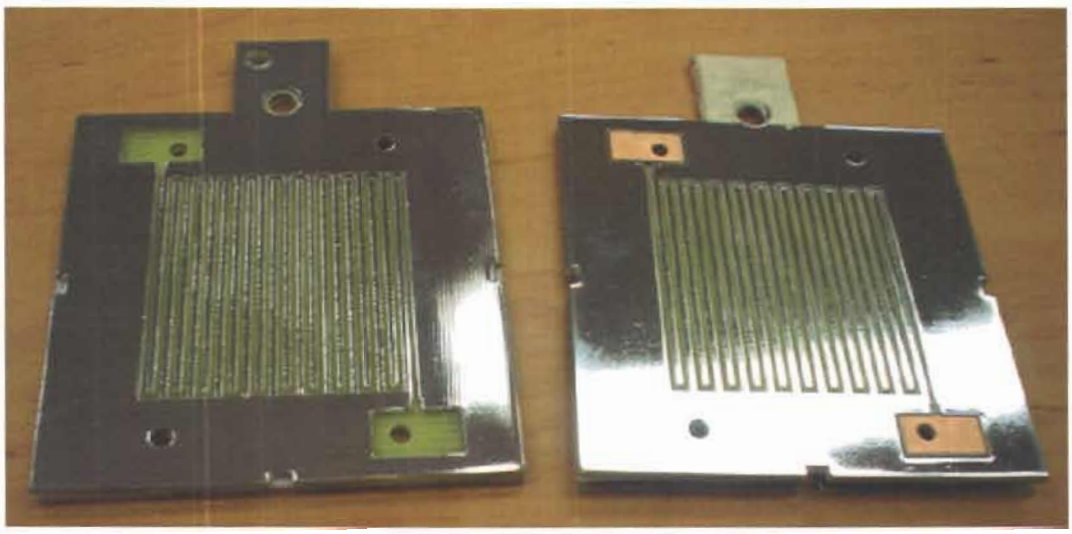

Figure 11 PCB BPs

A common problem that occurs when assembling a PEMFC stack is the deformation of the gasket material which blocks the flow channels and leads to the leakage of reactant gases from one side of the cell to the other side.

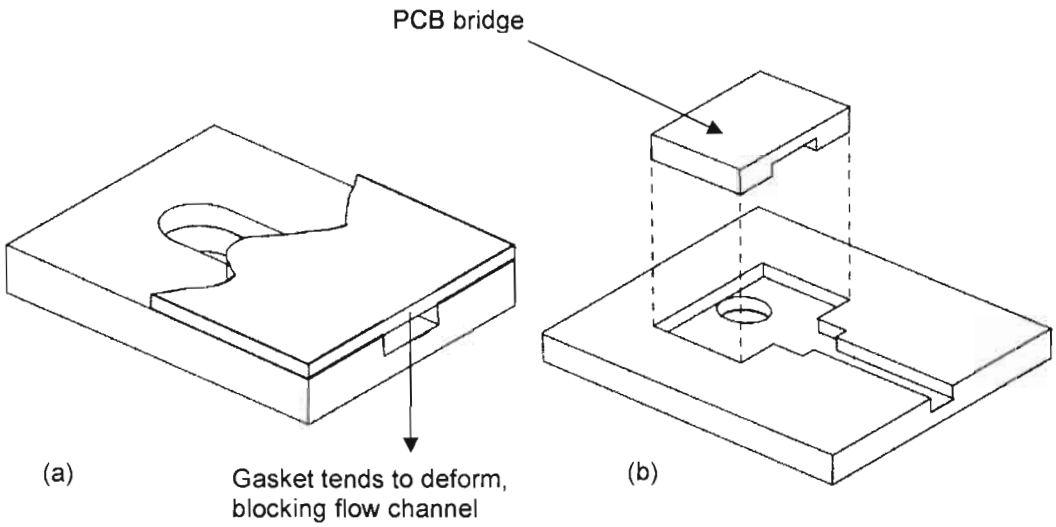

Figure 12 Gasket deformation

The situation is shown in figure 12(b). A solution to the problem in shown in figure 12(b). This was implemented by machining a separate bridge piece, also from PCB, and embedding it in the flow channel. This then serves as a support for the gasket, preventing it from deforming, while still allowing gas flow underneath it.

3.1.2 Membrane electrode assembly

Nafion 112 membranes were chosen for the construction of the PEMFC stack. These membranes have a thickness of only 50 μm, which contributes to the ease of water management within the cell and thus contributes to better cell performance under dryer conditions since back-diffusion of water from the cathode to the anode occurs more easily in thinner membranes. The membrane had an active area of 50 mm x 50 mm and was mounted in a supporting frame the same size as that of the BPs. The active area had a platinum loading of 0,5 $mg.cm^{-2}$ which is standard for FCs using air as an oxidant. When pure oxygen is used, the amount of platinum can be reduced further. Higher platinum loadings would result in slightly better cell performance, but at a higher cost. Figure 13 shows an example of a membrane electrode assembly (MEA) used.

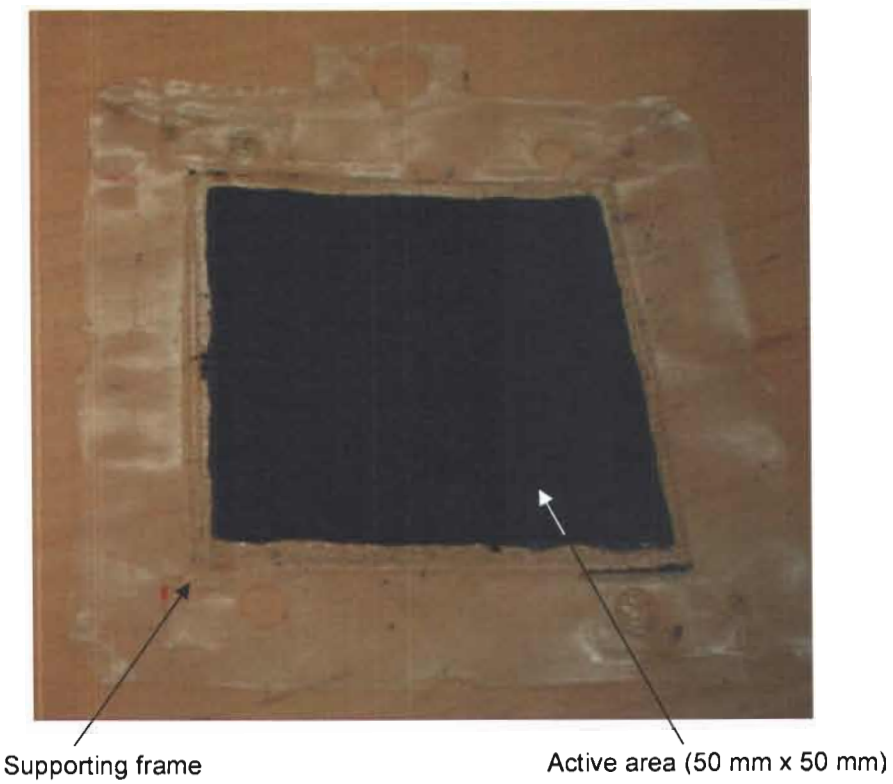

Figure 13 Nafion 112 membrane electrode assembly

3.1.3 Gas diffusion layers and gaskets

For the GDLs, ELAT® carbon cloth was used. The GDL had dimensions of 55 mm x 55 mm with a thickness of 0,5 mm. The dimensions were chosen to be slightly more than that of the membrane active area since in earlier prototypes it was found that a GDL with the same dimensions or smaller can damage the membrane or increase the probability of fuel crossover. Since cell flooding occurs more easily in thin diffusion layers (Schmitz *et al.* 2003:166), the chosen thickness of 0,5 mm was considered adequate in preventing water from blocking oxygen transport to the membrane. These GDLs were supplied as standard with the MEAs. Figure 14 shows the GDLs as well as the gaskets used.

In experiments performed by Schmitz *et al.* (2003:164), it was found that a GDL thickness of 1,05 mm produced the best cell performance. This can be attributed to an increase in contact pressure with a resulting decrease in contact resistance. However, the thickness of the gaskets used by them is unknown and it was decided to use a gasket material that has a thickness less than that of the GDL for this design. This would result in more pressure being exerted on the GDL which would decrease the contact resistance between the BPs, GDL and MEA. An incompressible PTFE gasket with a thickness of 0,25 mm was used.

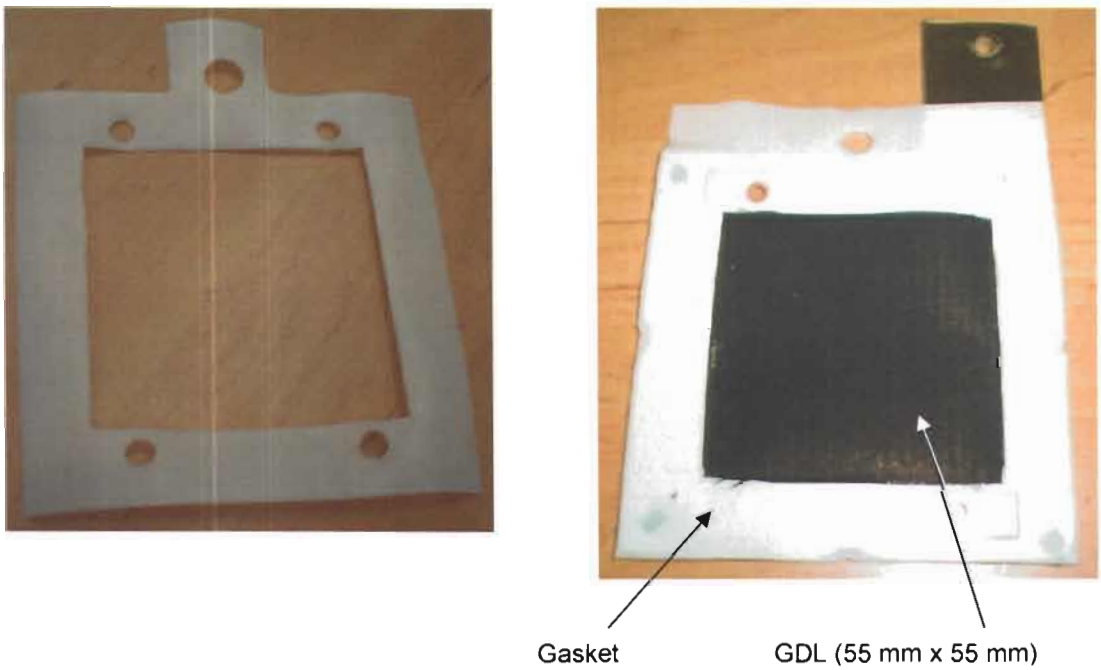

Figure 14 Gaskets and GDLs

Since the electrical resistance between the various cell components depends on the contact pressure on the components, it is important that a uniform contact pressure exists between the BPs, GDLs and the MEA. To measure the contact pressure, the MEA of a single cell was replaced by a pressure sensitive film. This film contains microcapsules filled with ink. As more pressure is applied to the film, more of these capsules break open and release their ink resulting in darker colors in areas of more pressure. The color variation can then be compared to a predefined index to determine the exact pressure exerted on a specific location. In this case, however, it was only necessary to observe the pressure distribution without knowing the exact pressure. Figure 15 shows this measured contact pressure at a bolt toque of 13 N.m. It can be seen from the figure that an even pressure is exerted over the entire membrane area. It was also found that larger stacks required a higher bolt torque in order to prevent leaks.

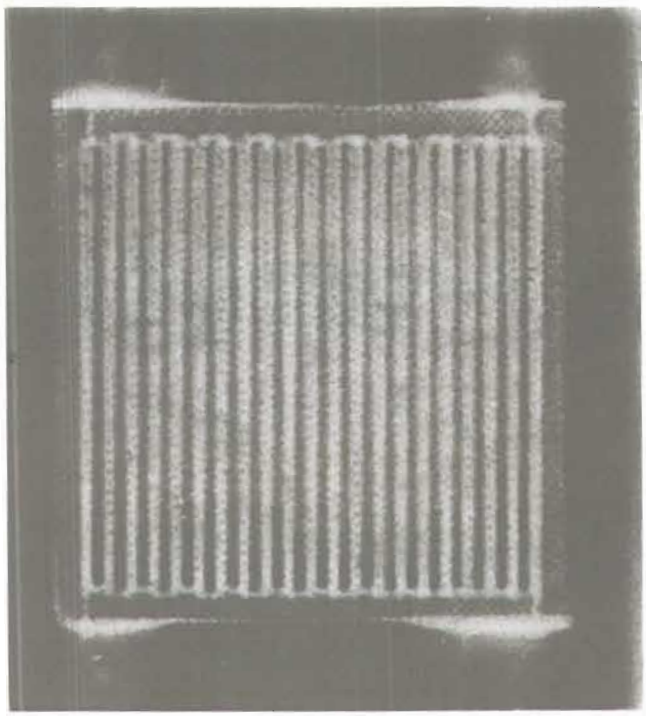

Figure 15 Pressure exerted by GDL on the MEA

An incompressible PTFE gasket was used since it was found in earlier prototypes that less rigid gasket materials, like silicon, tended to deform and resulted in more severe leaks and blockages.

3.1.4 Final stack assembly

The photograph in Figure 16 shows a completed two-cell stack. Figure 17 shows one end of the PEMFC stack. The GDL, surrounded by a gasket, is placed on top of the flow plate which is then followed by the MEA. The assembly shown in figure 17 is then followed by a bipolar plate as shown in figure 18. This is then followed by the components shown in figure 17, but in reverse order, to complete a two-cell stack. At both ends of the stack are stainless steel endplates which are used to ensure adequate and uniform contact pressure between the cell components. The entire stack assembly is compressed together using six bolts at a torque of 15 N.m.

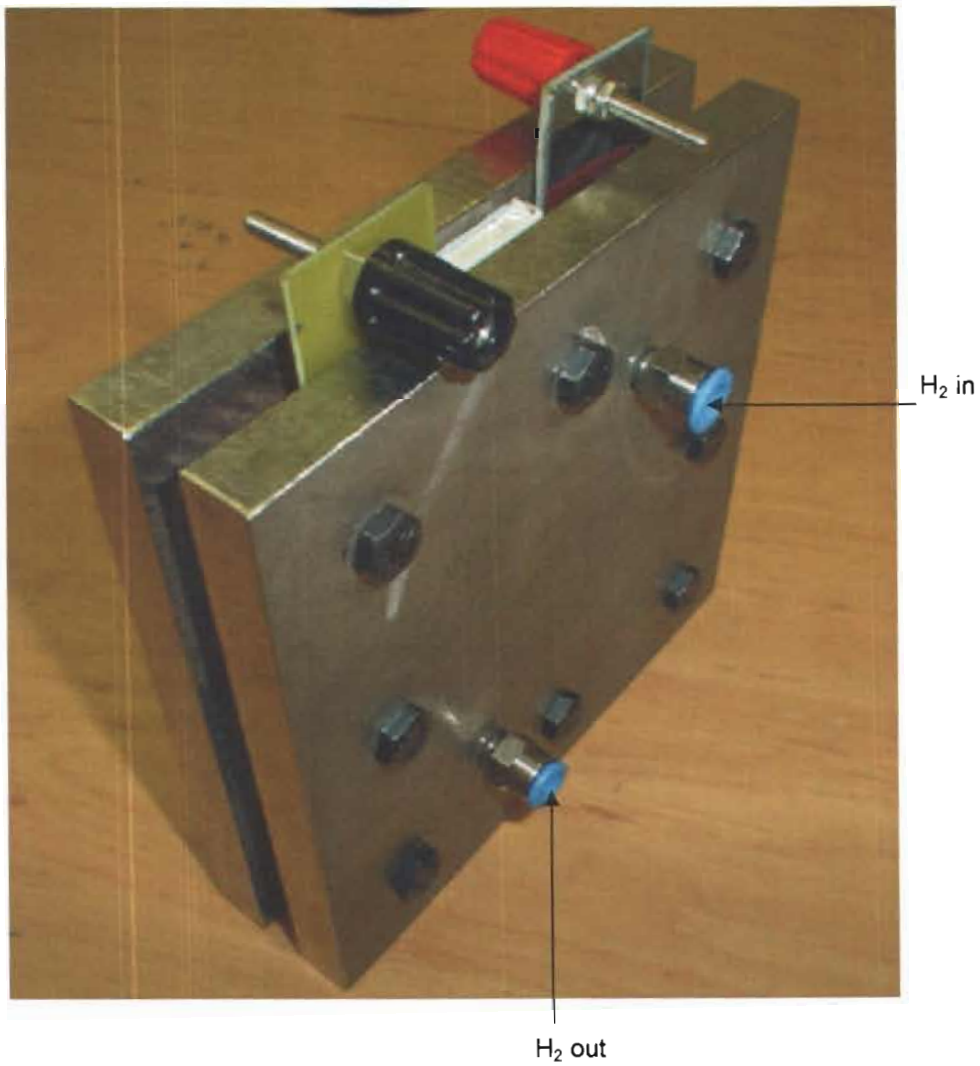

Figure 16 Assembled FC stack

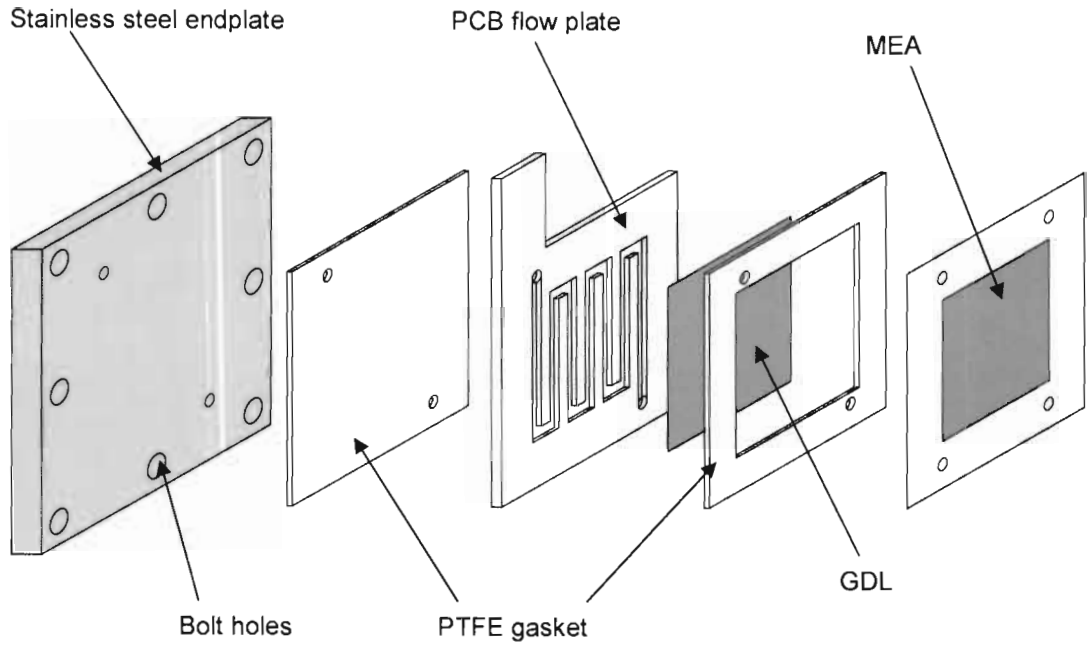

Figure 17 One end of a FC stack

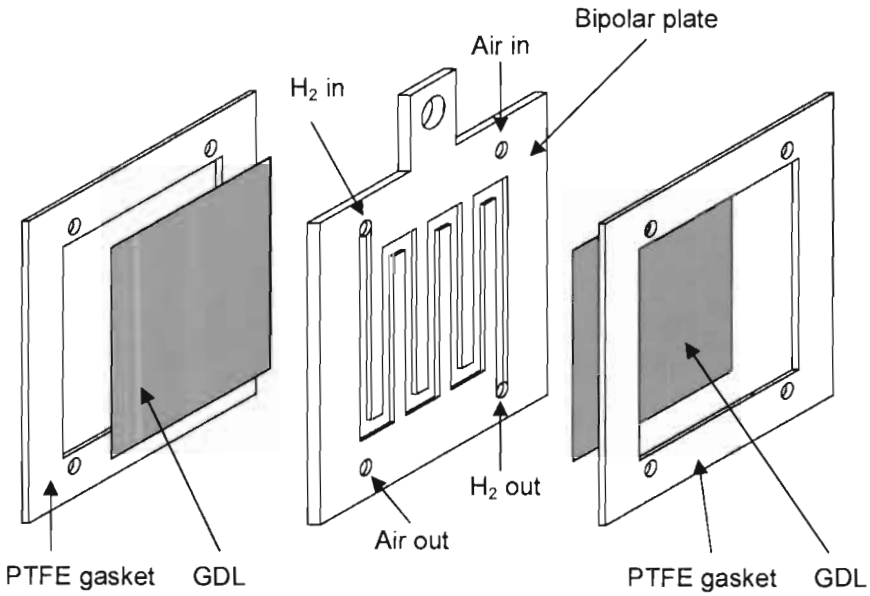

Figure 18 Bipolar plate assembly

3.2 Mathematical model of a 100 W PEMFC stack

In order to finalize the electronic circuit model of a FC stack as discussed in section 2.5, a small two-cell stack was constructed according to the method outlined in the previous section of this chapter. This stack was then used to obtain a polarization curve experimentally. The resulting data were used to calculate the constants of equation (2.21). The parameters needed for the electronic circuit model were then calculated by comparing equations (2.21) and (2.27). Both the mathematical model and electronic circuit equivalent were tested by comparing the predicted results with that obtained by testing a four-cell stack. After this, the model was adapted for a 100 W stack and used in the simulation of the final UPS system. The following table shows the output voltage of a two-cell stack at different currents:

Table 2 Measured data of a two-cell stack

	Stack voltage (V)	Current (A)	Current ($mA.cm^{-2}$)
1	1,82	0,1	4
2	1,76	0,2	8
3	1,75	0,3	12
4	1,73	0,4	16
5	1,72	0,5	20
6	1,70	0,6	24
7	1,69	0,7	28
8	1,68	0,8	32
9	1,67	0,9	36
10	1,65	1,0	40
11	1,61	1,5	60
12	1,57	2,0	80
13	1,53	2,5	100
14	1,50	3,0	120
15	1,46	3,5	140
16	1,42	4,0	160
17	1,38	4,5	180
18	1,33	5,0	200
19	1,26	5,5	220
20	1,23	6,0	240
21	1,16	6,5	260
22	1,09	7,0	280
23	1,01	8,0	320

From the above data, it can be seen the open circuit voltage of the two cell stack, NE_{OC}, is equal to 1,97 V. This means that the open circuit voltage of a single cell would be equal to 0,985 V. By substituting values from table 2 into equation (2.21), with N_C = 2, the values of r, A and m can be calculated. A typical value of 0,008 cm^2mA^{-1} was used for n. Points 1, 3, 12, 16, 22 and 23 was substituted for i (in $mA.cm^{-2}$) and V_{STACK} in the equation,

$$V_{STACK} = N_C E_{OC} - N_C ri - N_C A\ln(i) - N_C me^{ni} \text{ V} \qquad (N_C=2) \tag{3.1}$$

resulting in six equations :

$$\begin{aligned}
8r &+ 2{,}7726A + 2{,}0650m &= 0{,}15\\
24r &+ 4{,}9698A + 2{,}2015m &= 0{,}22\\
160r &+ 8{,}7641A + 3{,}7930m &= 0{,}40\\
320r &+ 10{,}1503A + 7{,}1933m &= 0{,}55\\
560r &+ 11{,}2696A + 18{,}7867m &= 0{,}88\\
640r &+ 11{,}5366A + 25{,}8716m &= 0{,}96
\end{aligned}$$

The above equations can be written in matrix form :

$$\mathbf{A}x = \mathbf{b} \tag{3.2}$$

Where

$$\mathbf{A} = \begin{matrix} 8 \\ 24 \\ 160 \\ 320 \\ 560 \\ 640 \end{matrix} \begin{matrix} 2{,}7726 & 2{,}0650 \\ 4{,}9698 & 2{,}2015 \\ 8{,}7641 & 3{,}7930 \\ 10{,}1503 & 7{,}1933 \\ 11{,}2696 & 18{,}7867 \\ 11{,}5366 & 25{,}8716 \end{matrix}, \quad x = \begin{matrix} r \\ A \\ m \end{matrix} \quad \text{and} \quad \mathbf{b} = \begin{matrix} 0{,}15 \\ 0{,}22 \\ 0{,}40 \\ 0{,}55 \\ 0{,}88 \\ 0{,}96 \end{matrix}$$

To solve for the solution matrix, x, equation (3.2) can be rewritten in the form

$$x = \mathbf{A}^{-1}\mathbf{b}$$

The above equation was solved using MATLAB, and the following values were found :

r = 0,0006 $k\Omega.cm^2$

A = 0,0351 V

m = 0,0147 V

These results were verified by substituting the values of N_C, r, A, m and n back into equation (3.1) and a graph was drawn, using MATLAB, of the voltages calculated using the model. The graph in figure 19 shows both the measured values (red curve) and calculated values (blue curve). It can be seen that the model accurately matches the measured data.

From the measured data in table 2, it can be seen that at a cell voltage of about 0,5 V, which is a typical operating voltage of a FC, the current is 8 A. This is equivalent to a power output of 4 W per cell. A 100 W stack would thus require 25 cells. To obtain a mathematical model of a 100 W stack, a value of N_C = 25 can be substituted in equation (3.1). Together with the calculated values of r, A, m and n, this equation then becomes :

$$V_{STACK} = 25(0,986) - 25(0,0003)i - 25(0,0351)\ln(i) - 25(0,0147)e^{0,008i} \text{ V}$$

$$\therefore V_{STACK} = 24,65 - 0,0075i - 0,8775\ln(i) - 0,3675e^{0,008i} \text{ V} \quad (3.3)$$

Equation (3.3) only holds true when i is given in terms of current density (mA.cm^{-2}). The equation of a four-cell stack would be:

$$V_{STACK} = 3,944 - 0,0012i - 0,1401\ln(i) - 0,0588e^{0,008i} \text{ V}$$

3.3 Electronic circuit equivalent model of a 100 W PEMFC stack

An electronic circuit model for a PEMFC stack was discussed in chapter two. To evaluate the accuracy of this model, it will be compared against the measured and calculated data of a two-cell stack from the previous section. Once the accuracy of the model has been verified, it can be adapted to represent a 100 W stack.

The equation relating the output voltage and current of the circuit in figure 6 can be given by

$$V_O = V_S - V_{BE} - I_O R2 - nV_T \ln\left(\frac{I_O}{I_{SD}}\right) - R1 \cdot I_S e^{\frac{I_O R2}{V_T}} \text{ V} \quad (3.4)$$

or

$$V_O = V_S + nV_T \ln(I_{SD}) - V_{BE} - I_O(\mathrm{R2} + \mathrm{R_D}) - nV_T \ln(I_O) - \mathrm{R1} \cdot I_S e^{\frac{I_O \mathrm{R2}}{V_T}} \ \mathrm{V} \qquad (3.5)$$

where the thermal voltage, V_T, is 25 mV at room temperature. V_O is the output voltage and I_O the load current drawn from the stack. In order to finalize the circuit model, the following values must be determined from equation (3.5) :

- V_S (voltage of the battery).
- R1 and R2.
- The emission coefficient of the diode, *n*.
- Saturation current of the diode, I_{SD}.
- Saturation current of the two transistors, I_S.
- Ohmic resistance of the diode (R_D).

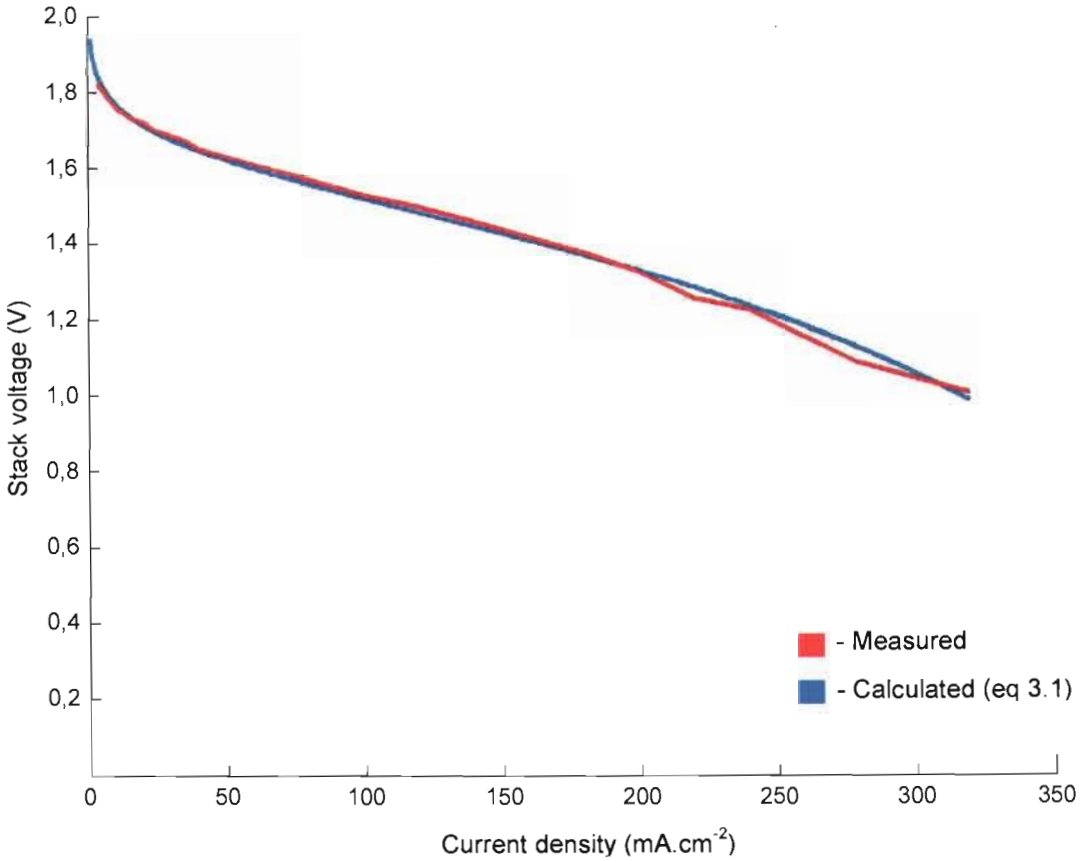

Figure 19. Calculated and measured V-I curve of a two-cell stack.

It is important to note that equation (3.4) expresses the cell voltage in terms of the current in Amperes. Equation (3.1), however, uses milliamperes per surface area (cm^2) as the unit for the cell current. In order to compare these two equations, equation (3.1) must be converted to also express the current in units of Amperes. It is know that the output voltage of a two-cell stack can be given by :

$$V = 2(0,986) - 2(0,0003)i - 2(0,0351)\ln(i) - 2(0,0147)e^{0,008i} \text{ V}$$

Knowing that a current of 8 A correspond to a current density of 320 $mA.cm^{-2}$ the new value of *r*, for example, can be calculated :

$$2(0,0003)(320) = 0,192$$
$$\therefore 2r(8) = 0,192$$
$$\therefore r = 0.012\ \Omega$$

The new value of n was calculated in the same way :

$$e^{0,008(320)} = 12,936$$
$$\therefore e^{8n} = 12,936$$
$$\therefore n = \frac{\ln(12,936)}{8}$$
$$\therefore n = 0,32\ A^{-1}$$

The unit of *m* and *A* is volts, and their values can stay the same. The equation for a two-cell stack, using amperes as the unit of current, then becomes :

$$V = 2(0,986) - 2(0,012)I_O - 2(0,0351)\ln(I_O) - 2(0,0147)e^{0,32I_O} \text{ V}$$

The graph in figure 20 shows the cell voltage given by the equation above and the measured cell voltage. It can be seen from the above graph that there is a constant difference of 0,26 V between the calculated voltage and the measured voltage. This is because of the current that appears in the ln-term in equation (3.1). This current value cannot be changed from $mA.cm^{-2}$ to A while still keeping the same form of equation (3.1). The model can however be adapted by just subtracting a constant difference of 0,13 V per cell. This constant voltage difference can be

compared to the V_{BE} term of equation (3.5). The voltage for a two-cell stack can thus be calculated using

$$V_{STACK} = 2(0,986) - 2(0,012)I_O - 2(0,0351)\ln(I_O) - 2(0,0147)e^{0,32I_O} - 2(0,13)\text{ V}$$

$$\therefore V_{STACK} = 1,972 - 0,26 - 0,024I_O - 0,07\ln(I_O) - 0,0294e^{0,32I_O}\text{ V} \quad (3.6)$$

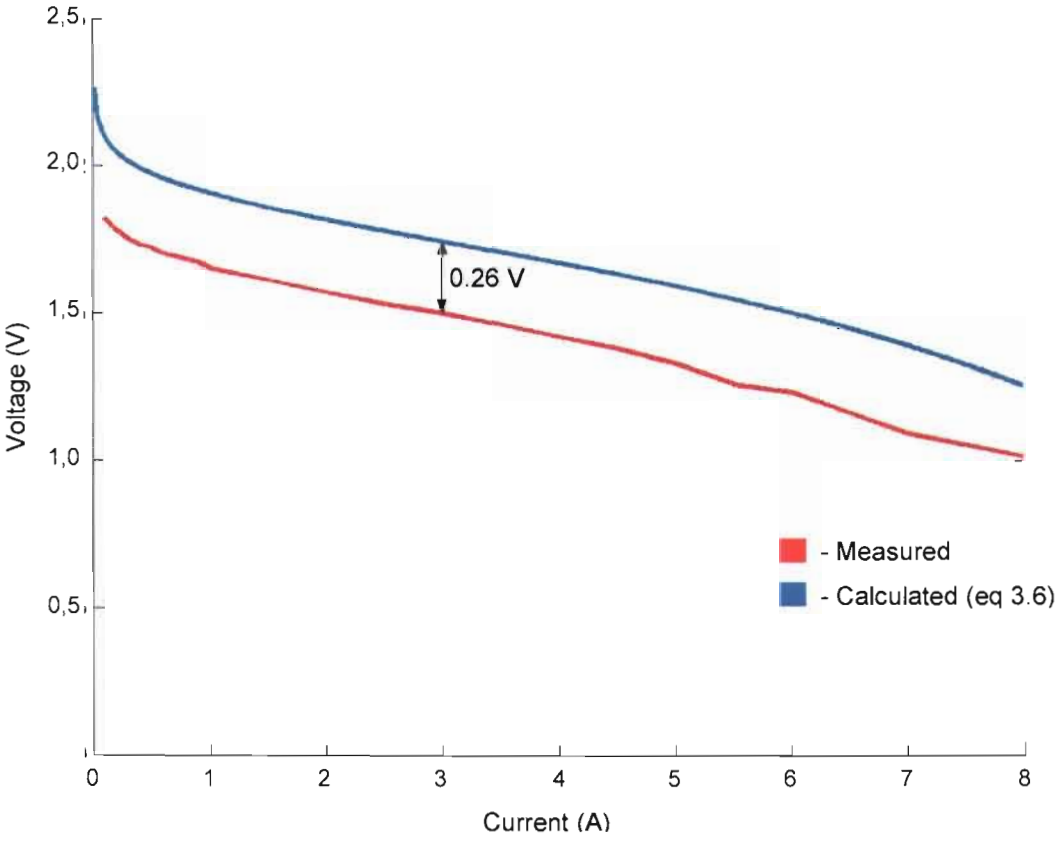

Figure 20 Polarization curve of a two-cell stack in terms of current

The values of equation (3.5) can be calculated by comparing it with the above equation and establishing the following relationships :

$V_S + nV_T \ln(I_{SD}) = 1,972$, where V_S is the theoretical output voltage of 2,46 V,

$$(R2 + R_D) = 0,024$$

$$nV_T = 0,07$$

$$R1.I_S = 0,0294$$

$$\frac{R2}{V_T} = 0,32$$

A value for R1 was chosen as 10 Ω. The values of equation (3.5) were then calculated to be :

- R2 = 0,008 Ω
- I_S = 0,00294 A
- n = 2,8 ≈ 3
- R_D = 0,016 Ω
- I_{SD} = 0,000938 A

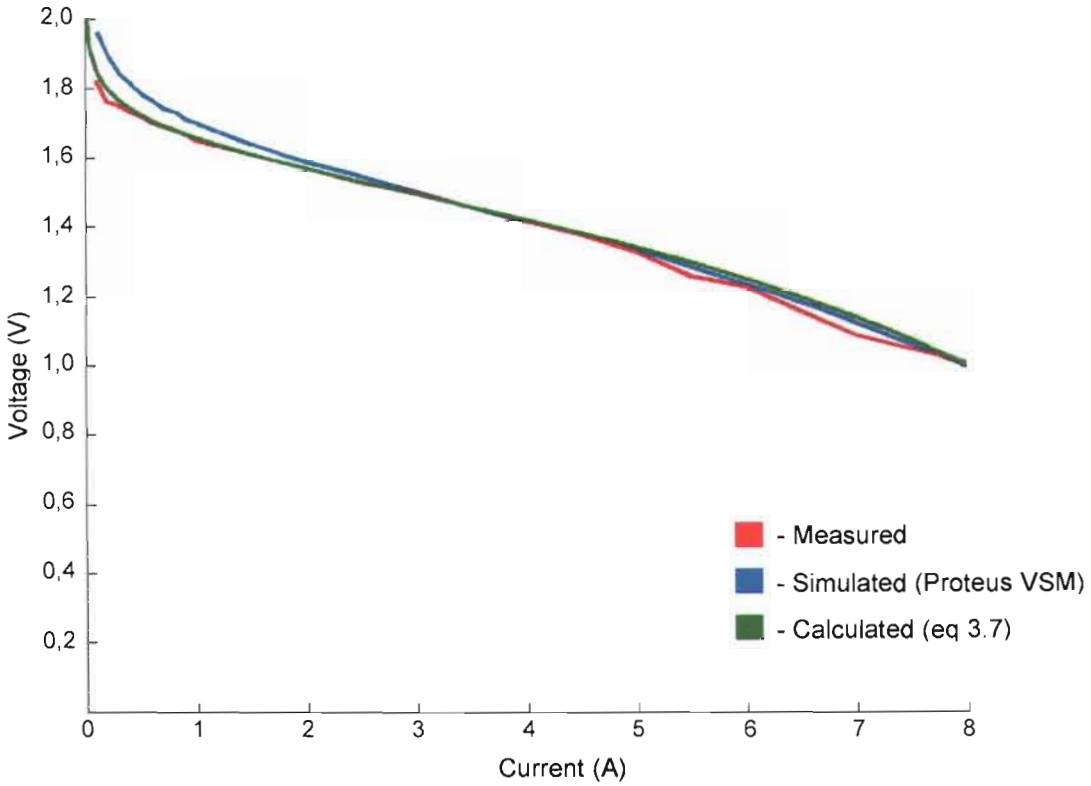

Figure 21 Measured, simulated and calculated V-I curve of a two-cell stack

The above values were used to change the SPICE models of the transistors and the diode of the circuit in figure 6. The circuit was simulated using the Proteus VSM , SPICE-based, software package. The graph in figure 21 shows the measured-, simulated-, and calculated output voltage of a two-cell stack. It can be seen from figure 21 that the simulated and calculated data correspond very well to the actual measured data, especially in the operating range of the FC stack. The final mathematical equations for a two-cell stack, four-cell stack, and 100 W stack are as follows :

two-cell stack : $V_{STACK} = 1{,}972 - 0{,}26 - 0{,}024I_O - 0{,}07\ln(I_O) - 0{,}0294e^{0{,}32I_O}$ (3.7)

four-cell stack : $V_{STACK} = 3{,}944 - 0{,}52 - 0{,}048I_O - 0{,}1404\ln(I_O) - 0{,}0588e^{0{,}32I_O}$ (3.8)

100 W stack : $V_{STACK} = 24{,}65 - 3{,}25 - 0{,}3I_O - 0{,}8775\ln(I_O) - 0{,}3675e^{0{,}32I_O}$ (3.9)

The component values for the electronic circuit equivalent models of the two-cell stack, four-cell stack and 100 W stack are summarized in table 3.

Table 3 Parameters for an electronic circuit model

Value	Two-cell stack	Four-cell stack	100 W stack
R1 (Ω)	10	10	10
R2 (Ω)	0,008	0,008	0,008
n	3	6	35
I_{SD} (A)	0,000938	0,000938	0,000957
R_D (Ω)	0,016	0,04	0,292
I_S (A)	0,00294	0,00588	0,03675

3.4 Design of a DC-DC boost converter

A FC / capacitor hybrid system can be used in cases where the load power changes constantly in either a predictable or unpredictable manner, as in telecommunication systems. In such a hybrid system, the FC operates close to its maximum power at all times. When the power requirements from the load is low, the FC charges the batteries or capacitors. When the load requires more power, even higher than the FC's maximum power, energy is taken from the EES

devices (Larmine and Dicks 2003:362-364). Figure 22 shows a configuration of a hybrid system using supercapacitors (Choi *et al* 2005:2).

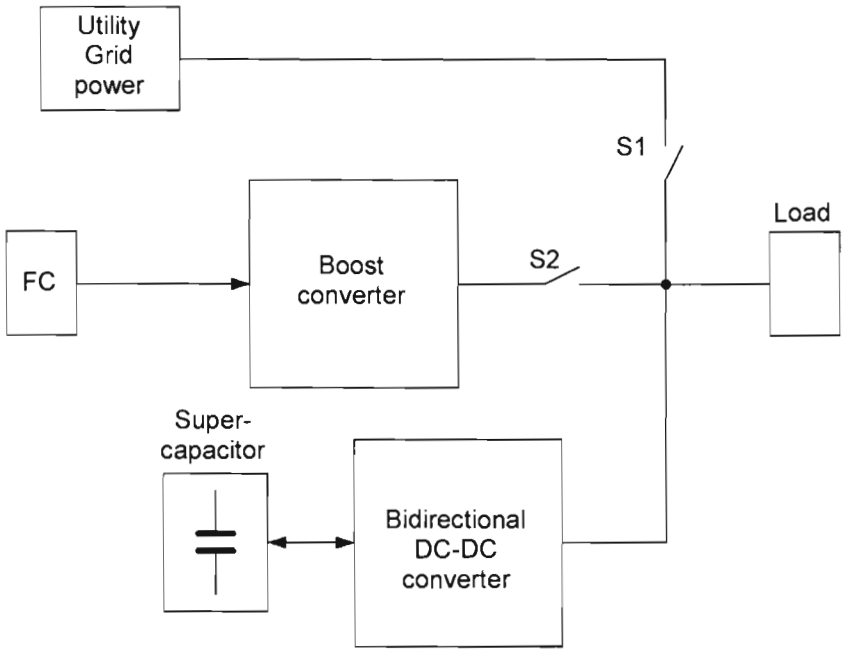

Figure 22 Hybrid system configuration

In the proposed system above, the switch S2 is open under normal conditions when power from the utility grid is available. When grid power is available, the supercapacitor is charged via the bidirectional converter. When the grid power fails (in effect, switch S1 opens), switch S2 is closed by a supervisory control system, air and hydrogen begins to flow through the stack, and the FC stack begins to operate. It takes a certain amount of time however for the membrane to become fully humidified and for the stack to reach its maximum power. During this time, the supercapacitor discharges via the bidirectional converter to supply energy to the load.

3.4.1 Determining the size of the supercapacitor

The energy stored in a capacitor with a voltage rating V and a capacitance C is given by :

$$W = \frac{1}{2}CV^2 \text{ J} \tag{3.10}$$

It can be seen that the energy stored in a capacitor is directly proportional to the square of the voltage. A drop of 30 percent of the voltage represents a release of 50 percent of the stored energy (Choi *et al.* 2005:6). Assuming a typical FC startup time of maximum 20 seconds and a load requiring 100 W of power, the amount of energy can be calculated using

$$\begin{aligned} \Delta W &= Pt \\ &= (111)(20) \\ &= 2220 \text{ J} \end{aligned} \tag{3.11}$$

Note that a power of 111 W was used. This is to compensate for the losses in the converter, assuming that the converter has an efficiency of 90 percent. This means that the size of the capacitor must be such that it will release 50 percent of its stored energy (2220 J) as its voltage drops from a value V_C to $0,7V_C$ (a drop of 30 percent). Assuming a working voltage of 10 V, the required capacitance can be calculated :

$$\begin{aligned} &\frac{1}{2}CV_C^2 - \frac{1}{2}C\left(0,7V_C^2\right) = 2220 \\ &\therefore \frac{1}{2}C\left(V_C^2 - 0,7V_C^2\right) = 2220 \\ &\therefore C = \frac{4440}{V_C^2 - 0,7V_C^2} = \frac{4440}{(10)^2 - (7)^2} = 87 \text{ F} \end{aligned} \tag{3.12}$$

Since the actual voltage rating of most commercially available supercapacitors is 2,5 V, the above design would require the series connection of four 350 F supercapacitors.

3.4.2 Design of a switch mode boost converter

This section will first discuss the design of a 12 W switch mode boost converter together with the required digital PID control system. Since the same controller can be used for a 100 W converter, only some component values will change from that of the 12 W design. These values are calculated using the same formulae and will be given at the end of this section. The converter will be designed with regard to the following specifications :

- Output power (P_{OUT}) = 12 W
- Output voltage (V_{OUT}) = 12 V
- Maximum output current (I_{OUT}) = 1 A

- Input voltage (V_{IN}) = 5 V (V_{IN_MIN}) to 7 V (V_{IN_MAX})
- Output voltage ripple limited to 1 percent (ΔV_{OUT} = 0,12 V)

The same design procedure as used in Choi *et al.* (2005:6) will be used to calculate the values of the PWM switching frequency and capacitor (C_1) as shown in figure 23. An inductor value of 330 µH was chosen. Resistors R_1 and R_2 are used as a voltage divider to scale the feedback voltage to a level suitable for the ADC of the PIC microcontroller. These values were chosen so that an output voltage of 12 V will result in a feedback voltage of 2,5 V (half of the range of the ADC converter).

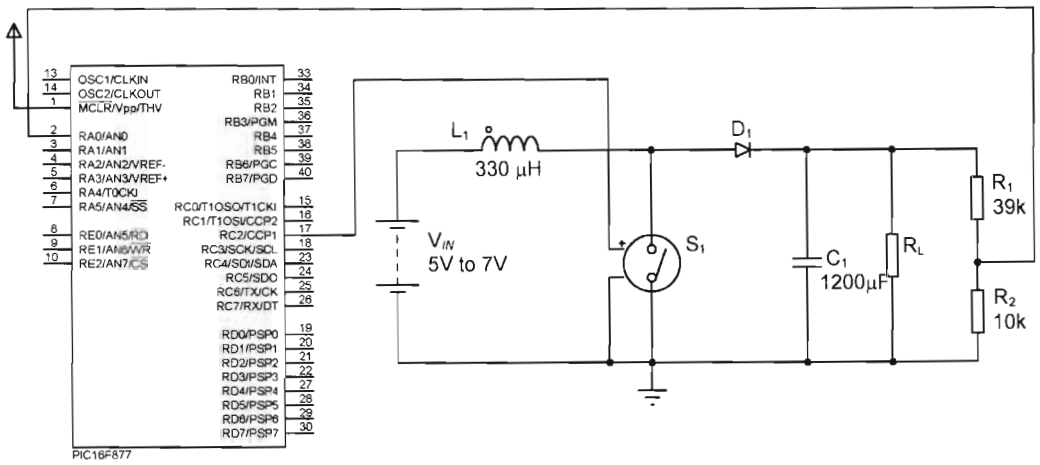

Figure 23 Complete 12 W boost converter circuit

$$\text{Maximum voltage conversion ratio : } M = \frac{V_{OUT}}{V_{IN\_MIN}} = \frac{12}{5} = 2,4 \qquad (3.13)$$

$$\text{Maximum input current : } I_{IN\_PEAK} = \frac{P_{OUT}}{V_{IN\_MIN}} = \frac{12}{5} = 2,4\ \text{A} \qquad (3.14)$$

Switching frequency:

$$F_S = \frac{V_{OUT}(M-1)}{10(0,1I_{OUT})(L1)(M^3)} = \frac{(12)(1.4)}{10(0,1)(330x10^{-6})(2.4)^3} = 3,68x10^3\ \text{Hz} \qquad (3.15)$$

Peak current through switch :

$$I_{SW\_PEAK} = I_{OUT}\left[M + \left(\frac{V_{OUT}}{2 \cdot F_S \cdot I_{OUT} \cdot L1}\right)\left(\frac{M-1}{M^3}\right)\right] = 2{,}5\ \text{A} \tag{3.16}$$

Peak voltage across switch :

$$V_{SW\_PEAK} = V_{IN\_MAX} + V_{OUT} = 7 + 12 = 19\ \text{V} \tag{3.17}$$

$$C_1 = \frac{L1\left(I_{SW\_PEAK}\right)^2}{2 \cdot \Delta V_{OUT} \cdot \left(V_{OUT} - V_{IN\_MIN}\right)} = 1227\ \mu\text{F} \tag{3.18}$$

A value of 1200 μF was chosen for C_1. Figure 24 shows the final prototype that was used to test the converter and the control system.

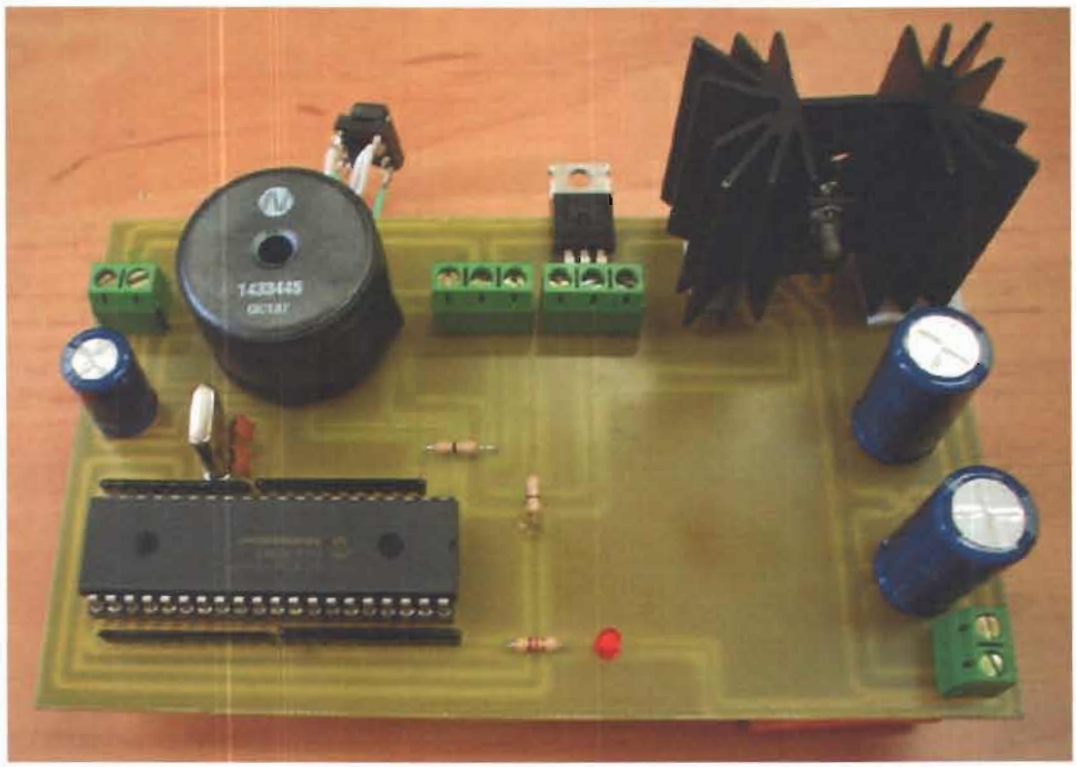

Figure 24. Assembled switch mode boost converter.

The open circuit voltage of a 25-cell stack, calculated earlier in this chapter, was found to be 24,65 V. The stack will be operated at a voltage of 0,5 V per cell, resulting in a stack output voltage of 12,5 V. The UPS load is assumed to require a voltage 48 V. For the design of the boost converter, the following specifications were used :

- Output power (P_{OUT}) = 100 W
- Output voltage (V_{OUT}) = 48 V
- Maximum output current (I_{OUT}) = 2,08 A
- Input voltage (V_{IN}) = 12,5 V (V_{IN_MIN}) to 24,65 V (V_{IN_MAX})
- Output voltage ripple limited to 0,5 percent (ΔV_{OUT} = 0,24 V)

The value of L_1 was chosen as 330 μH. The voltage divider (R_1 and R_2) should have an output voltage of 2,5 V when the converter output voltage is 48 V. The values of R_1 and R_2 were calculated to be 18 kΩ and 1 kΩ respectively. The value of the capacitor C_1 was calculated as 1580 μF. A value of 1800 μF was used in the final design. Finally, the switching frequency was calculated to be 3,5 kHz.

The digital PID controller was implemented in software using the PIC microcontroller with a clock frequency of 4 MHz. The feedback voltage is measured using its built-in ADC while the PWM switching signal will be generated by the PIC's PWM module. The software program written for the PIC is given in Annexure 1 (adapted from Ibrahim 2002:217-218). The duty cycle of the PWM signal is limited to 80 percent to ensure stable operation of the converter. For a sampling time of T seconds, the PIC algorithm used can be summarized as follows (Ibrahim 2002196-197):

BEGIN

DO FOREVER

Get set point : $r(kT)$

Get system output : $y(kT)$

Calculate error : $e(kT) = r(kT) - y(kT)$

Calculate integral term : $p(kT) = be(kT) + p(kT - T)$

Calculate differential term : $q(kT) = ce(kT) - ce(kT - T)$

Calculate PID output : $u(kT) = p(kT) + ae(kT) + q(kT)$

IF $u(kT) >$ MAX

$p(kT) = p(kT - T)$

$u(kT)$ = MAX

ELSE IF $u(kT) <$ MIN

p(kT) = $p(kT - T)$

u(kT) = MIN

END IF

Send control signal to PWM module to change duty cycle

Save variables : $p(kT - T) = p(kT)$

$e(kT - T) = e(kT)$

Wait for next sample

END DO

END

The constants in the above algorithm can be calculated by :

$$a = k_p \qquad b = \frac{k_p T}{T_j} \qquad c = \frac{k_p T_D}{T}$$

where the sampling time, T, is equal to 1 ms and :

$$k_p = \frac{1.2T_1}{KT_d} \qquad T_j = 2T_d \qquad T_D = 0.5T_d$$

The values of K, T_1 and T_d were chosen as 134, 0,01 s and 0,0001 s respectively.

3.5 Summary

This chapter considered the design and construction of a PEMFC stack as well as a switch mode boost converter. Both the mathematical model and electronic circuit equivalent of a PEMFC stack were finalized and it was found that these models closely represented experimental data. Both models were then adapted for a four-cell stack as well as a 100 W stack consisting of 25 cells. The models of the four-cell stack are compared against experimental data in the next chapter in order to determine if the proposed models can be accurately used to predict the performance of PEMFC stack of any size. The electronic circuit equivalent model obtained for a 100 W stack is then used in a simulation, together with the 100 W boost converter, to determine the operation of the final system.

Chapter 4 Measurements and results

The previous chapter presented designs of a PEMFC stack, electronic circuit model of a FC stack and a switch mode boost converter. In order to determine the accuracy with which the performance of a PEMFC stack of any size can be predicted, the performance of a four-cell stack will be compared against that obtained using the proposed model. The four-cell stack will also be used to determine the effects that various operating conditions have on the performance of a PEMFC. The stack will be tested under conditions of varying humidity and reactant gas flow rates. The experimental setup and equipment used in these tests will also be discussed. Measurements taken from the 12 W boost converter will be compared with simulated values in order to evaluate the design of the converter. Finally, the simulation results of a 100 W PEMFC stack and converter will be discussed.

4.1 Fuel cell test equipment

In chapter two, the various factors that have an effect on the performance of PEMFCs were discussed. This section will explain how the effects of humidity and reactant gas flow rate can be measured. The diagram in figure 25 shows the experimental setup used to test the performance of a PEMFC.

Pure hydrogen (99,999 percent purity) is supplied from a pressurized cylinder through a pressure regulator. A pressure of no more than 50 kPa was applied at either the anode or cathode of the FC in order to prevent possible damage to the membranes. The hydrogen flow rate was controlled with a needle valve and the mass flow rate measured with a digital mass flow meter (DMFM). A flashback arrestor was used at the hydrogen input port to prevent possible damage to the test equipment in the event of hydrogen combustion. Hydrogen was circulated through the stack and the unused gas vented out into the atmosphere.

Air needed by a PEMFC stack can be supplied by various devices, including compressors, fans and blowers. The power requirements for these devices can be quite high. Other disadvantages including low efficiencies and unreliable operation make these devices especially unsuited for small FCs of under 200 W. Diaphragm pumps are widely used in gas sampling equipment, chemical processing and fish tank aerators and have the following advantages (Larmine and Dicks 2003:329) :

- Low cost

- Silent
- Reliable for long-term continuous operation
- Wide variety of sizes available
- Consumes little power
- Efficient

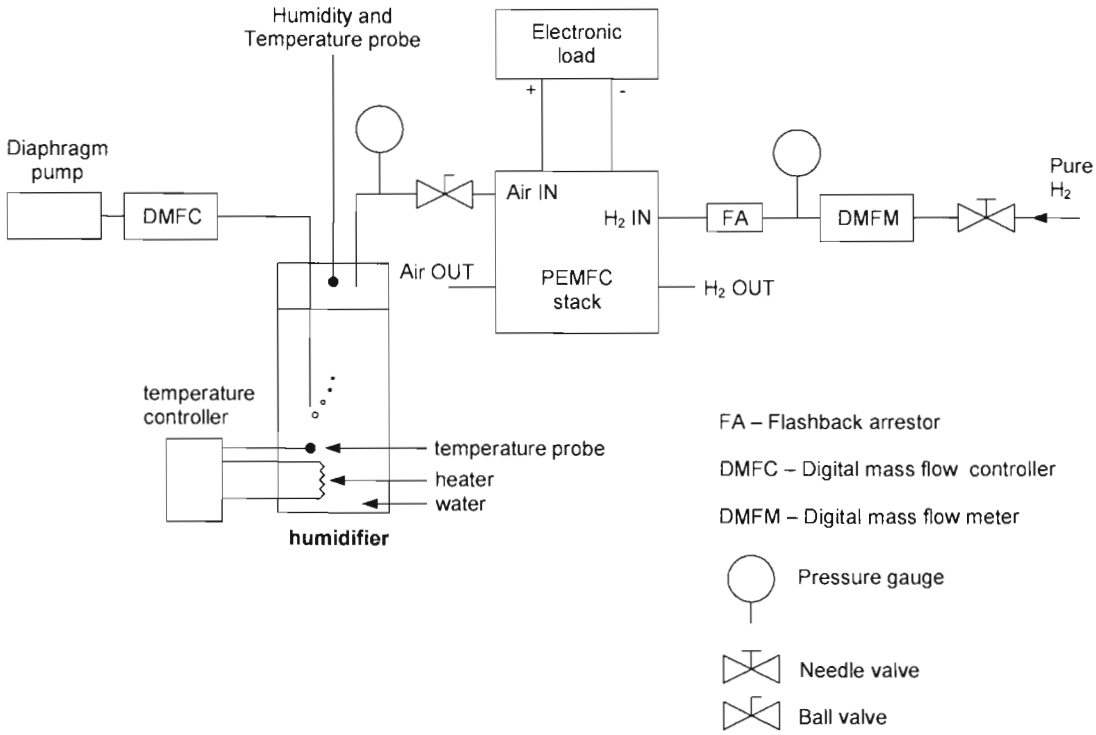

Figure 25 Experimental setup for FC testing

A fish tank aerator was initially used for FC testing because of its low cost and adequate operating pressure of 0,2 kPa. This pump was later replaced with a commercial air pump containing air filters to ensure the supply of clean air to the FC stack. The air flow rate was maintained at a constant level using a digital mass flow controller. The air was humidified using a bubble humidifier in which air is bubbled through heated water. The humidity level can be controlled by controlling the temperature of the water. Heating the air also contributes to heating the cell, resulting in higher performance. The temperature and humidity of the air was measured using a humidity probe, placed inside the humidifier. The humidifier can be seen on the left-hand side in figure 26.

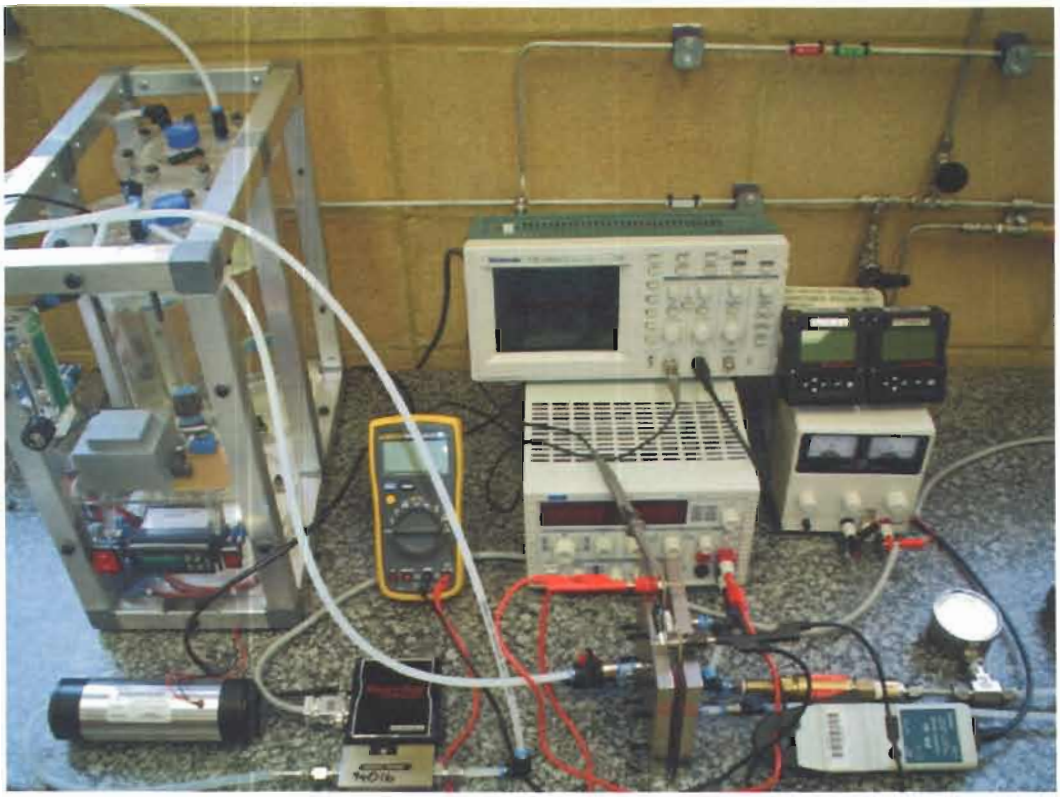

Figure 26 Fuel cell test setup

Figure 27 Fuel cell during operation

According to the FC reaction

$$2H_2 + O_2 \rightarrow 2H_2O$$

exactly two moles of hydrogen are needed to react with one mole of oxygen. The relationship between the amounts of chemical reactants and products is called stoichiometry (Kotz and Treichel 2003:122). Reactants are often supplied at rates higher than the stoichiometric balance, especially when air is used as the oxidant. According to the basic PEMFC equation given above, four electrons are transferred for each mole of oxygen so that

$$\text{charge} = 4\ F \times \text{moles of } O_2$$

In the above equation, F is the charge of one mole of electrons (96 485 C). Since current is defined as the rate of the flow of electric charge, the above equation can be rewritten as

$$O_2 \text{ usage} = \frac{I}{4F} \text{ moles.s}^{-1}$$

for a single cell. For a stack comprising of n cells, the equation would be

$$O_2 \text{ usage} = \frac{nI}{4F} \text{ moles.s}^{-1} \qquad (4.1)$$

If the voltage of each cell in an n-cell stack is V_{CELL}, then the power of the stack (P_{STACK}) can be expressed as

$$P_{STACK} = V_{CELL} \cdot n \cdot I \text{ W} \qquad \therefore I = \frac{P}{nV_C} \text{ A} \qquad (4.2)$$

Substituting the above into equation (4.1) :

$$O_2 \text{ usage} = \frac{P_{STACK}}{4 \cdot V_{CELL} \cdot F} \text{ moles.s}^{-1}$$

Since the molar mass of oxygen is 32 $g.mol^{-1}$, the oxygen usage can be written in terms of kg per second :

$$O_2 \text{ usage} = 8{,}29x10^{-8} \cdot \frac{P_{STACK}}{V_{CELL}} \ kg.s^{-1}$$

Oxygen is normally supplied as part of air. The molar proportion of air that is oxygen is 0.21 and the molar mass of air is $28{,}97x10^{-3}$ $kg.mole^{-1}$. The air usage of a FC stack can then be given as

$$\text{Air usage} = 3{,}57x10^{-7} \cdot \frac{P_{STACK}}{V_{CELL}} \ kg.s^{-1}$$

or in terms of standard liters per minute (SLPM) :

$$\text{Air usage} = 18{,}2x10^{-3} \cdot \lambda \cdot \frac{P_{STACK}}{V_{CELL}} \ \text{SLPM}, \qquad (4.3)$$

for a stiochiometry of λ. The hydrogen flow rate required (with a stiochiometric rate of λ) can be calculated in the same way. A FC stack with an output power of P_{STACK} and a voltage of V_{CELL} per cell would require a hydrogen flow rate of

$$H_2 \text{ usage} = 7{,}5x10^{-3} \cdot \lambda \cdot \frac{P_{STACK}}{V_{CELL}} \ \text{SLPM}. \qquad (4.4)$$

For a four-cell PEMFC stack delivering an output power of 16 W (P_{STACK}), with each cell having a voltage of 0,5 V (V_{CELL}), the required hydrogen and air flow rates can be calculated as :

$$\text{Air usage} = 18{,}2x10^{-3}(2)\frac{16}{0{,}5} = 1{,}165 \ \text{SLPM and}$$

$$H_2 \text{ usage} = 7{,}5x10^{-3}(2)\frac{16}{0{,}5} = 0{,}48 \ \text{SLPM}.$$

The above equations are based on a stiochiometric rate of two (λ=2). Higher flow rates prevent fuel starvation and helps with water management inside the cell by pushing excess water out more rapidly. In the experimental measurements the air flow rate was controlled with the DMFC, while the hydrogen flow rate was adjusted with a needle valve and measured with a DMFM.

4.2 Performance of a 16 W PEMFC stack

This section will consider the performance of a four-cell stack that was built using the design given in chapter three. The performance of the stack will be compared with a mathematical model and electronic circuit equivalent of the stack.

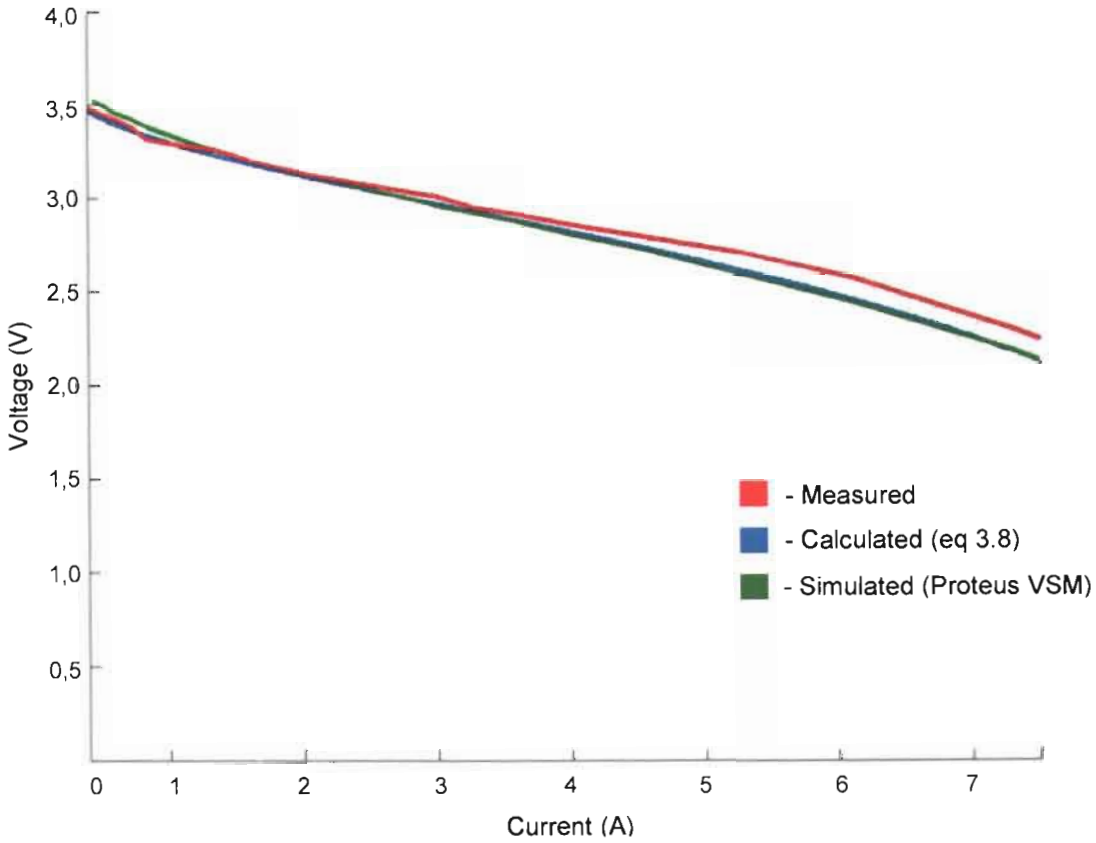

Figure 28 Performance curves of a 16 W PEMFC stack

The following operational parameters were used in testing the stack :

- Air pressure = 0,2 kPa

- Hydrogen pressure = 0,2 kPa
- Air flow rate = 1,17 SLPM
- Hydrogen flow rate = 0,48 SLPM
- Air humidity = 100 percent
- Hydrogen humidity = 0 percent
- Ambient temperature was measured to 24 °C.

The graph in figure 28 shows the measured polarization curve of the stack together with the simulated and calculated curves. It can be seen that the measured curve closely resembles the calculated and simulated ones, confirming that both models can accurately predict the performance of a PEMFC stack of any size. Small deviations can be attributed to the changing of operating conditions like temperature, humidity as well as reactant gas flowrates and pressure for which the models don't compensate.

After a few weeks of operation (not continious), a slight performance decrease was observed for the 16 W stack. Upon disassembling the stack, no visible sign of corrosion of the BPs were observed. A white substance was found on the cathode side of one of the membranes and its GDL as shown in figure 29.

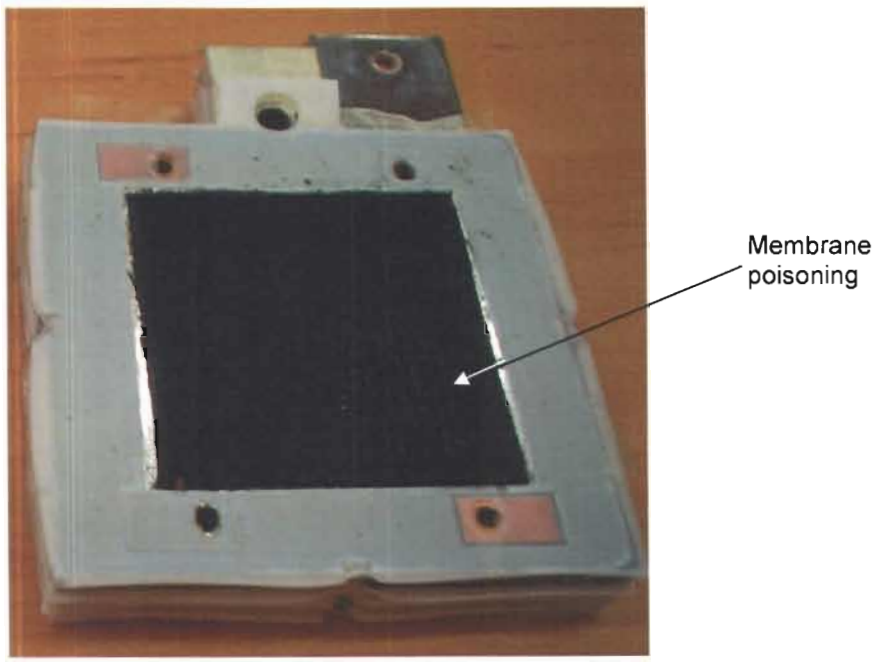

Figure 29. Membrane poisoning

Although there were no visible signs of corrosion on the electrode associated with the defective membrane, it could be possible that corrosion took place on a microscopic scale. A possible reason could be that flaws existed on the chrome layer which allowed mobile copper ions to leach out onto the membrane and resulted in a decrease in effective active area and the associated decrease in cell performance. The exact cause of the membrane poisoning is outside the scope of this research and is left for future study. A major concern regarding the series interconnection of FCs to form a stack is that if one cell fails, the performance of the entire stack decreases.

The start up time of the FC stack was measured by first applying a 4 A load to the stack and then opening the valves to allow reactants to the stack while recording the stack voltage with an oscilloscope. The voltage of the stack over time as shown in the graph of figure 30 shows the start-up characteristics of a four-cell stack. It took 7,5 seconds for the stack to reach a constant output voltage. As the size of a PEMFC stack increases, the startup time will also increase.

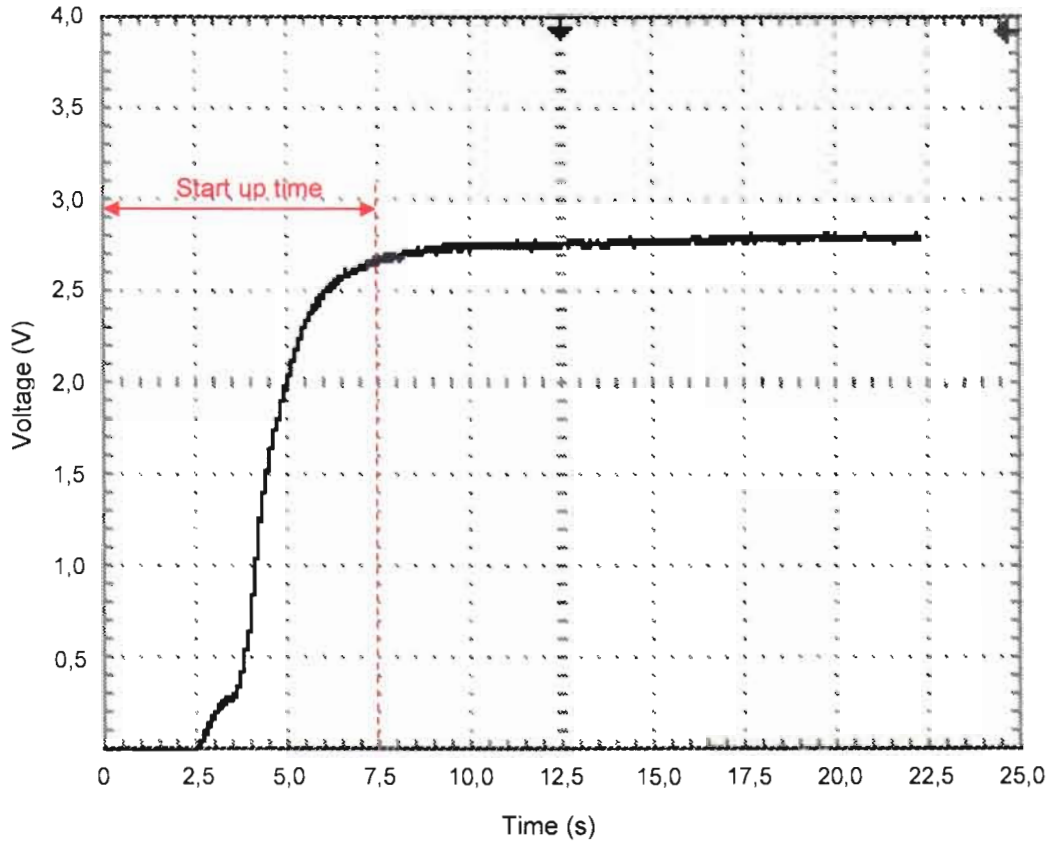

Figure 30 Startup time of a 16 W PEMFC stack

4.3 Performance of a 12 W boost converter

Section 3.4.2 in the previous chapter detailed the design of a 12 W switch mode boost converter. The converter should provide a constant output voltage of 12 V regardless of a change in input voltage (provided it remains in the range of 5 V to 7 V) or load current. The converter was tested by first varying the input voltage and measuring the output voltage at full load (output current of 1 A). This graph of output voltage and input voltage against time is given in figure 31. The graph shows that in spite of a change in input voltage, the output voltage stays at a constant 12 V. This means that when connected to a FC stack, a constant output voltage will be maintained even if the stack voltage varies.

Next, the input voltage was kept at a constant level and the load current was varied between 0 A to 1 A while measuring the converter output voltage for input voltages of 5 V and 7 V. The resulting graphs in figure 32 and figure 33 show that the output voltage stays at a constant level as the load current changes.

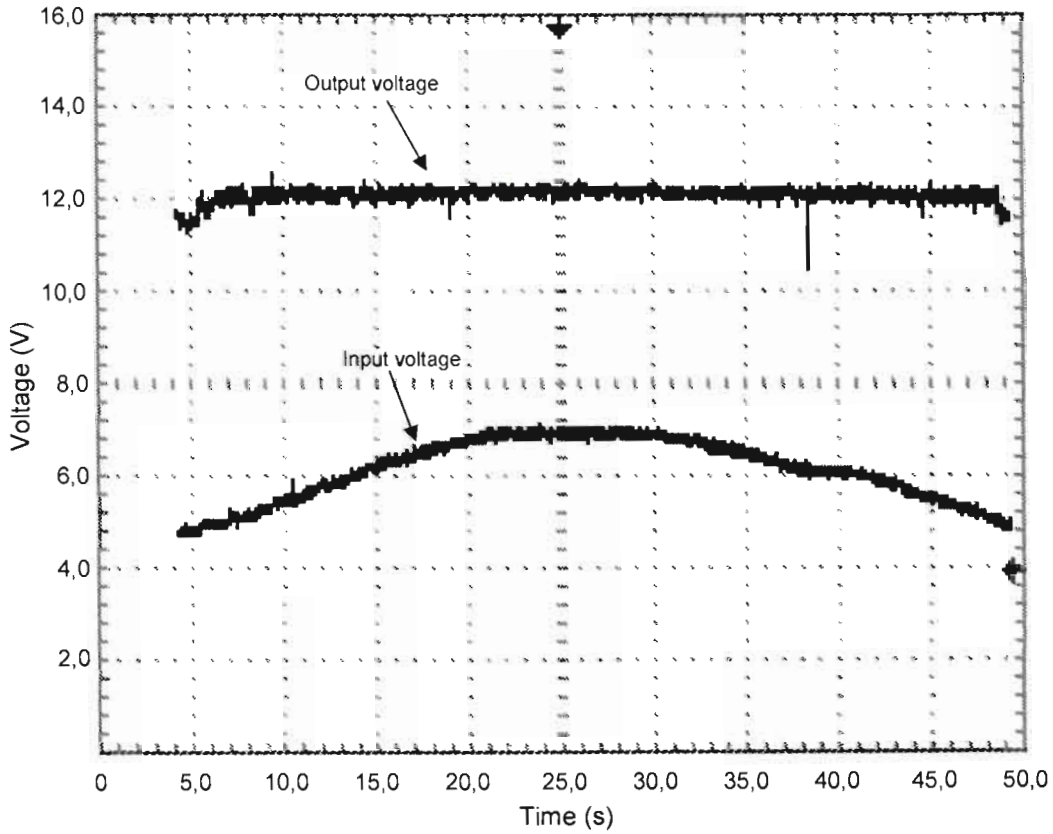

Figure 31 Output voltage of boost converter with changing input voltage.

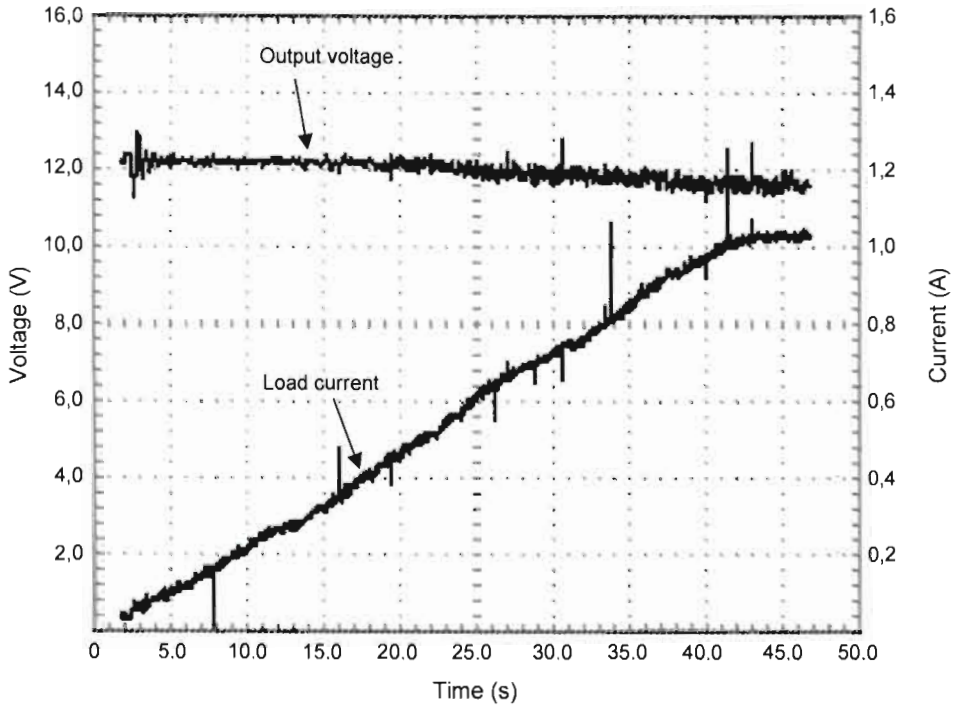

Figure 32 Output voltage of converter with varying load current (V_{IN} = 5V)

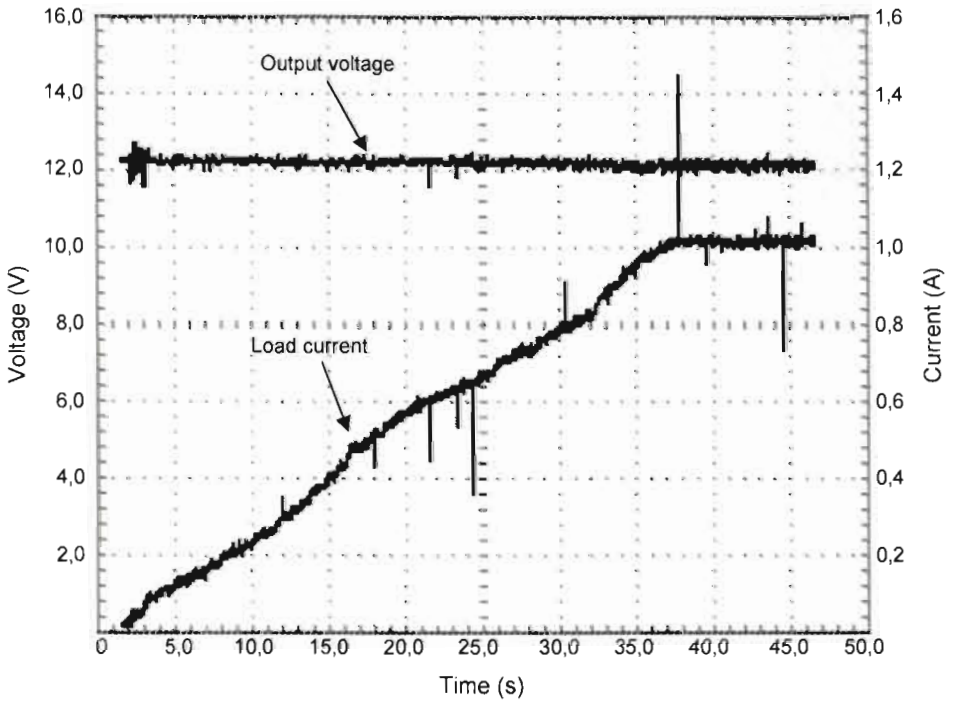

Figure 33 Output voltage of converter with varying load current (V_{IN} = 7V)

4.4 Simulation results of 100 W stack and converter

The diagram in figure 34 shows an equivalent electronic circuit of a 100 W PEMFC stack connected to a switch mode boost converter. The simulation of this circuit provides more insight on how the FC and boost converter interact. It is known that as the load current increases, the output voltage of the FC will drop. In spite of this, a constant voltage of 48 V has to be maintained at the controller output.

The graph in figure 35 shows the output of the converter / FC combination under various load currents. The output voltage of the FC is also shown. It can be seen that the converter output voltage stays at a constant level of 48 V. Of course, since the efficiency of a practical converter is around 85 percent, a FC stack with an output power of more than 100 W will be needed when driving a 100 W load.

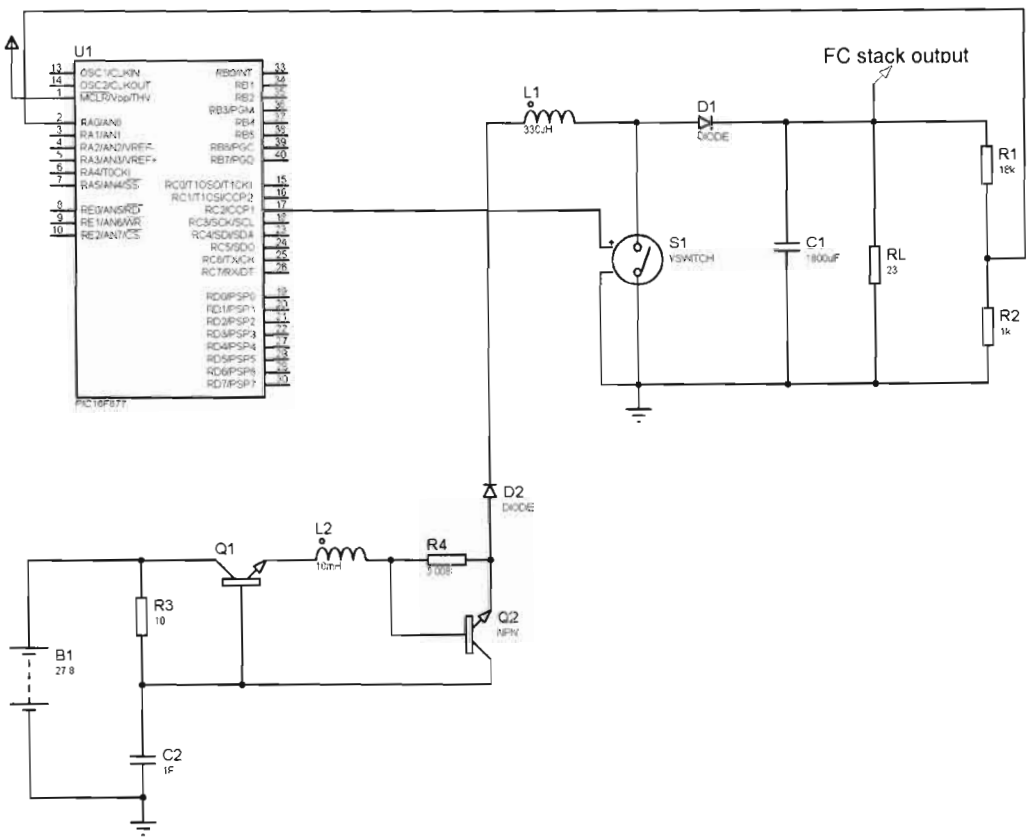

Figure 34 Complete circuit diagram of PEMFC stack and boost converter

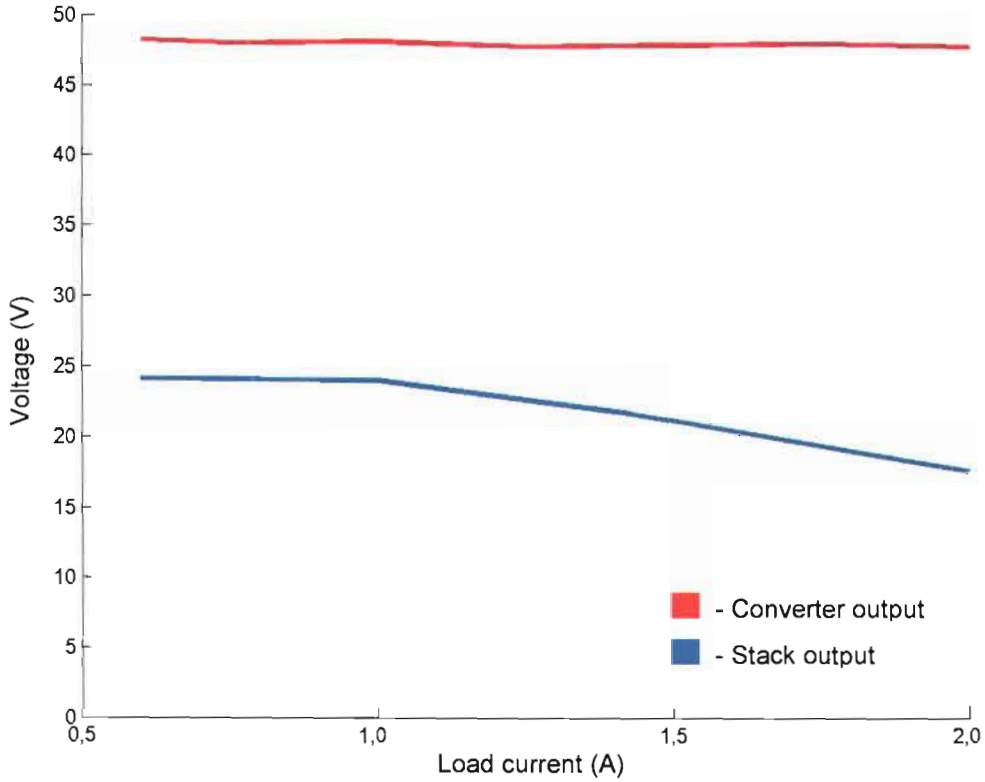

Figure 35 Simulation results of boost converter connected to a PEMFC stack

4.5 Summary

The performance characteristics of a 16 W PEMFC stack together with the equipment used to obtain these results were presented in this chapter. It was observed that the measured performance closely resembled simulated results, proving that the proposed model is indeed a viable way of predicting PEMFC performance.

Measurements were also performed to determine the operation of a switch mode boost converter using a digital PID controller. The characteristics of the converter were determined under conditions of varying input voltage and changes in load current. Finally, simulation results were shown for a 100 W PEMFC stack operating together with a boost converter.

Chapter 5 discusses conclusions that can be reached from the results of this research. Recommendations will also be made regarding future research on low-cost PEMFCs and their applications.

Chapter 5 Conclusions and recommendations

5.1 Introduction

This chapter discusses the conclusions that can be drawn from this research regarding low-cost PEMFCs, the use of power converters for FC power conditioning and using supercapacitors as EES devices in a PEMFC UPS system. Finally recommendations are made regarding future research that is still required regarding low-cost PEMFCs and their applications and possible alternatives to the proposed design.

5.2 Conclusions

It was found that PCB technology can be used in the manufacturing of low-cost PEMFC stacks. It is crucial however that these BPs be plated with protective coatings since copper electrodes were found to cause permanent damage to the MEA. It was shown that the lifetime of a FC stack using PCB BPs can be increased significantly by plating the copper areas with layers of nickel and chrome. Chrome plating is also a low-cost process and didn't make a significant contribution the the final cost of the design. The plating process must be of such a nature that no part of the underlying layers are exposed. It was suspected that membrane poisoning of one cell in a four-cell stack occurred due to possible plating defects on one of the BPs. Other sources of corrosion would have resulted in the poisoning of all the membranes in the stack. The fact that only one side of a single membrane was effected pointed to plating defects. Using PCB technology made it possible for BPs to be designed and manufactured in a few hours.

The performance of the proposed FC design showed that the cost of both the components and their manufacturing can be significantly reduced without a large sacrifice in performance. Cell voltages of up to 0.5 V at a current of 8 A were obtained. It was observed that a FC stack performed at higher levels on warmer days. Although the effects of temperature on FC performance were not experimentally verified, these observations confirm the influence of temperature on FC performance as described by Knights *et al* (2004:133). It can be concluded from this that environmental conditions around the FC stack must be carefully controlled in order to ensure long-term and efficient operation.

The importance of the way in which a cell was assembled has also been observed by measuring the contact pressure exerted by the cell components on the membrane. It was found that the

required torque of the bolts increased as more cells are added to a stack. By adding more cells to a stack, more reactant gas leaks appeared. By tightening the bolts further, these leaks dissapeared, however. From this it was concluded that maximum torque should be applied to the bolts when assembling a FC stack.

An equivalent circuit model of a PEMFC stack was investigated and found to be invaluable in predicting cell performance and designing peripheral electronic circuitry for PEMFCs. Measurements performed on an actual PEMFC stack closely resembled simulations performed on the equivalent circuit model. Although the basic outline of a circuit equivalent of a PEMFC stack was found in literature, no details regarding the design of such a circuit were given. In this study a method has been developed for the design of a FC circuit equivalent in order to predict the performance of a larger FC stack based on performance data of single cells or small stacks.

The VI characteristics of FCs confirmed the importance of using power converters to ensure a stable output voltage. The start-up time for a 16 W stack was measured to be 7.5 seconds. This showed the importance of including EES devices in a FC UPS design. The use of supercapacitors instead of batteries was further investigated and it was found that there were important advantages in replacing batteries with supercapacitors in a PEMFC UPS system.

5.3 Recommendations

- Although the circuit equivalent model of a FC stack proved to be accurate under constant stack operating conditions, it is still unable to predict the performance of a stack under changing conditions. The model should be expanded to allow the simulation of a PEMFC stack under varying conditions of pressure, humidity, temperature and reactant gas flow rates. The startup time of a FC is also very important and a future model should be able to predict the startup time of a stack consisting of any number of cells.

- It was found that although the cell components could be manufactured at low-cost and in little time, the final assembly of a stack was still a tedious process. In order to mass produce FC stacks using the proposed design, low-cost manufacturing processes still have to be designed or identified. Furthermore, other materials should be investigated for use as protective coatings on the PCB BPs. Although gold plating would be more expensive, it is suspected that it could increase the lifetime and performance of a PEMFC stack. It is also very important that a plating process is used that would result in an evenly coated surface.

- A major concern regarding the series interconnection of cells to form a FC stack is the fact that a failure of one cell would result in the entire stack becoming defective. The design of a modular PEMFC stack, in which single cells can be replaced as needed, should be investigated. It would also be beneficial if single cells can be added to a stack in order to increase its power output as demands increase.

BIBLIOGRAPHY

CHO, E.A., JEON, U.-S., HA, H.Y., HONG, S.-A. and OH, I.-H. 2004. Characteristics of composite bipolar plates for polymer electrolyte membrane fuel cells. *Journal of Power Sources,* 125:178-182.

CHOI, D.-K., LEE, B.-K., CHOI, S.-W., WON, C.-Y. and YOO, D.-W. 2005. A novel power conversion circuit for cost-effective battery-fuel cell hybrid system. *Journal of Power Sources*, 152:245-255.

CHU, H., YEH, C. and CHEN, F. 2003. Effects of porosity change of gas diffuser on performance of proton exchange membrane fuel cell. *Journal of Power Sources,* 123:1-9.

COSTAMAGNA, P. and SRINIVASAN, S. 2001. Quantum jumps in the PEMFC science and technology from the 1960s to the year 2000. Part I. Fundamental scientific aspects. *Journal of Power Sources*, 102(1-2):242-252, December.

COSTAMAGNA, P. and SRINIVASAN, S. 2001. Quantum jumps in the PEMFC science and technology from the 1960s to the year 2000. Part II. Engineering, technology development and application aspects. *Journal of Power Sources*, 102(1-2):253-269, December.

DYER, C K. 2002. Fuel cells for portable applications. *Journal of Power Sources*, 106:31-43, April.

GAMBURZEV, S. and APPLEBY, A.J. 2002. Recent progress in performance improvement of the proton exchange membrane fuel cell (PEMFC). *Journal of Power Sources,* 107:5-12.

GUVELIOGLU, G.H. and STENGER, H.G. 2005. Computational fluid dynamics modeling of polymer electrolyte membrane fuel cells. *Journal of Power Sources*, Article in press.

HEINZEL, A. HEBLING, C., MÜLLER, M., ZEDDA, M. and MÜLLER, C. 2002. Fuel cells for low power applications. *Journal of Power Sources*, 105(2):250-255, March.

HERMANN, A., CHAUDHURI, T. and SPAGNOL, P. 2005. Bipolar plates for PEM fuel cells: A review. *International Journal of Hydrogen Energy*, 30:1297-1302.

INOUE, G., MATSUKUMA, Y. and MINEMOTO, M. 2005. Effect of gas channel depth on current density distribution of polymer electrolyte fuel cell by numerical analysis including gas flow through gas diffusion layer. *Journal of Power Sources*, Article in press.

JAOUEN, F., HAASL, S., VAN DER WIJNGAART, W., LUNDBLAD, A., LINDBERGH, G. and STEMME, G. 2005. Adhesive copper films for an air-breathing polymer electrolyte fuel cell. *Journal of Power Sources*, 144:113-121.

JIANG, R. and CHU, D. 2001. Stack design and performance of polymer electrolyte membrane fuel cells. *Journal of Power Sources*, 93(1):25-31, February.

JIANG, R. and CHU, D. 1999. Comparative studies of polymer electrolyte membrane fuel cell stack and single cell. *Journal of Power Sources*, 80:226-234.

JIANG, R. and CHU, D. 1999. Performance of polymer electrolyte membrane fuel cell (PEMFC) stacks. Part I. Evaluation and simulation of an air-breathing PEMFC stack.

JORDAN, L.R., SHUKLA, A.K., BEHRSING, T., AVERY, N.R., MUDDLE, B.C. and FORSYTH, M. 2000. Diffusion layer parameters influencing optimal fuel cell performance. *Journal of Power Sources*, 86:250-254.

KNIGHTS, S.D., COLBOW, K.M., ST-PIERRE, J. and WILKINSON, D.P. 2004. Aging mechanisms and lifetime of PEFC and DMFC. *Journal of Power Sources*, 127:127-134.

KOTZ, J.C. and TREICHEL, P.M. 2003. *Chemistry and Chemical Reactivity.* USA:Thomson/Brooks/Cole.

LARMINE, J. and DICKS, A. 2003. *Fuel Cell Systems Explained.* Sussex. John Wiley and Sons.

LEE, S.-J., HSU, C.-D. and HUANG, C.-H. 2005. Analysis of fuel cell stack assembly pressure. *Journal of Power Sources*, Article in press.

MEACHAM, J.R., JABBARI, F., BROUWER, J., MAUZEY, J.L. and SAMUELSEN, G.S. 2005. Analysis of stationary fuel cell dynamic ramping capabilities and ultra capacitor energy storage using high resolution demand data. *Journal of Power Sources*, Article in press.

MURPHY, O., CISAR, A. and CLARKE, E. 1998. Low-cost light weight high power density PEM fuel cell stack. *Electrochimica Acta,* 43(24):3829-3840.

O'HAYRE, R., BRAITHWAITE, D., HERMAN, W., LEE, S., FABIAN, T., CHA, S., SAITO, Y. and PRINZ, F.B. 2003. Development of portable fuel cell arrays with printed-circuit technology. *Journal of Power Sources*, 124(2):459-472, November.

PRASANNA, M., HA, H.Y., CHO, E.A., HONG, S.-A. and OH, I.-H. 2004. Influence of cathode gas diffusion media on the performance of PEMFCs. *Journal of Power Sources,* 131:147-154.

SCHMIDT, H., BUCHNER, P., DATZ, A., DENNERLEIN, K., LANG, S. and WAIDHAS, M. 2002. Low-cost air-cooled PEFC stacks. *Journal of Power Sources*, 105(2):243-249, March.

SCHMITZ, A., TRANITZ, M., WAGNER, S., HAHN, R. and HEBLING, C. 2003. Planar self-breathing fuel cells. *Journal of Power Sources*, 118:162-171.

SCHOLTA, J., ESCHER, G., ZHANG, W., KUPPERS, L., JORISSEN, L. and LEHNERT, W. 2005. Investigation on the influence of channel geometries on PEMFC performance. *Journal of Power Sources*, Article in press.

SCHULZE, M., KNORI, T., SCHNEIDER, A. and GULZOW, E. 2004. Degradation of sealings for PEFC test cells during fuel cell operation. *Journal of Power Sources*, 127:222-229.

SCOTT, D.S. 2004. Fuelcells: chip of the future?. *International Journal of Hydrogen Energy,* 29:1089-1093.

SCOTT, D.S. 2004. Inside fuelcells. *International Journal of Hydrogen Energy*, 29:1203-1211.

SUN, H., LIU, H. and GUO, L.-J. 2005. PEM fuel cell performance and its two-phase mass transport. *Journal of Power Sources,* 143:125-135.

VENGATESAN, S., KIM, H.-J., CHO, E.A., JEONG, S.U., HA, H.Y., OH, I.-H., HONG, S.-A. and LIM, T.-H. Operation of a proton exchange membrane fuel cell under non-humidified conditions using thin cast Nafion membranes with different gas diffusion media. *Journal of Power Sources*, Article in press.

WAHDAME, B., CANDUSSO, D. and KAUFFMANN, J.-M. 2005. Study of gas pressure and flow rate influences on a 500 W PEM fuel cell, thanks to the experimental design technology. *Journal of Power Sources*, Article in press.

WILLIAMS, M.V., KUNZ, H.R. and FENTON, J.M. 2004. Operation of Nafion-based PEM fuel cells with no external humidification: influence of operating conditions and gas diffusion layers. *Journal of Power Sources,* 135:122-134.

WIND, J., SPÄH, R., KAISER, W. and BÖHM, G. 2002. Metallic bipolar plates for PEM fuel cells. *Journal of Power Sources*, 105(2):256-260, March.

WOOD, D.L., YI, J.S. and NGUYEN, T.V. 1998. Effect of direct liquid water injection and interdigitated flow field on the performance of proton exchange membrane fuel cells. *Electrochimica Acta,* 43(24):3795-3809.

YOON, Y.-G., LEE, W.-Y., PARK, G.-G., YANG, T.-H. and KIM, C.-S. Effects of channel and rib widths of flow field plates on the performance of a PEMFC. *International Journal of Hydrogen Energy*, 30:1363-1366.

ANNEXURE A PIC source code for PID controller

```
#include <16f874.h>
#device ADC=10
#fuses XT,NOWDT,NOPROTECT,NOLVP,NOBROWNOUT,PUT
#use delay(clock=4000000)


main( )
{
   float a, b, c, T, T1, Ti, Td, K, Kp, setPoint, rkt, LSB, ekt, pkt,
   qkt, ykt, ukt;
   float MAX, MIN, pkt1, ekt1, duty, duty_c;
   int dutyCycle;
   long int V0;

   setup_adc_ports( RA0_ANALOG );          // setup ADC
   setup_adc( ADC_CLOCK_INTERNAL );
   set_tris_a( 0b11111111 );

   setup_ccp1( CCP_PWM );                 // set PWM module and frequency
   setup_timer_2( T2_DIV_BY_1, 255, 1 );


   LSB = 5.0/1024.0;
   MIN = 0.0;
   MAX = 800.0;                             // limit duty cycle
   pkt1 = 100.0;
   ekt1 = 0.0;

   T = 0.001;
   T1 = 0.01;
   Td = 0.0001;
   K = 134;
   Ti = 2*Td;
   TD = 0.5*Td;
   Kp = 1.2*T1/(K*Td);
   a = Kp;
   b = Kp*T/Ti;
   c = Kp*TD/T;

   setPoint = 2.45;

   while( 1 )
   {
      set_adc_channel( 0 );              //get system output
      delay_us( 20 );
      V0 = read_adc( );

      ykt = V0 * LSB;
      rkt = setPoint;
```

```
        ekt = rkt-ykt;                  // calculate error
        pkt = b * ekt + pkt1;           // integral term
        qkt = c * (ekt-ekt1);           // differential term
        ukt = pkt + a*ekt + qkt;        // PID output
        duty = 500.0 + ukt;             // calculate new duty cycle

        if( duty > MAX )                // prevents integral windup
        {
           pkt = pkt1;
           duty = MAX;
        }
        else if( duty < MIN )
        {
           pkt = pkt1;
           duty = MIN;
        }

        dutyCycle = (long int)duty;
        set_pwm1_duty( dutyCycle );     // set new duty cycle

        pkt1 = pkt;                     // save variables
        ekt1 = ekt;

        delay_us( 500 );
    }
}
```